UNIVERSITÀ DEGLI STUDI DI PADOVA

Scuola di Ingegneria
Dipartimento di Ingegneria dell'Informazione
Corso di Laurea Magistrale in Bioingegneria

Tesi di Laurea

A new method to devise strategies for the visual field examination

Relatore: Prof.ssa Maria Pia Saccomani

Correlatori: Ing. Enea Poletti
Ing. Chiara Rui

Laureanda: Beatrice Martinelli

24 Febbraio 2020

A.A. 2019/2020

Firma laureando Firma relatore

...alla mia famiglia che mi ha supportato e sopportato,

alle mie amiche che sono state sempre presenti in questi anni,

a tutti gli amici fantastici conosciuti all'università

che porterò sempre nel cuore…

Overview

Introduction

This thesis is the result of a collaboration with CenterVue S.p.A. in the Research and Development (R&D) department.

CenterVue was founded in 2008 in the M31 incubator in Padua as a start-up. Over the years it has confirmed its leadership in the world market in the development of tools for prevention and early diagnosis of eye diseases.

Currently, the company has about 60 employees in Italy and 20 in the American headquarters. It exports products all over the world reinvesting most of its profits in research and development. Designing cutting-edge instruments for eye screening is the method to safeguard patients' eyesight from eye diseases.

Over the years, medical device products such as DRS, MAIA, COMPASS, EIDON etc. have been perfected and used for eye diagnostics. In 2014 CenterVue developed COMPASS, launched in the market in 2015.

COMPASS allows to carry out the perimetry examination, a fundamental ophthalmic test for the evaluation of the visual space width and of the light intensities perceived in the various points of the retina. This examination is used to diagnose the alterations or deficits in the visual field caused by diabetes, glaucoma, and other retinal diseases. The role played by this examination is especially important in the diagnosis and monitoring of glaucoma, as this pathology causes a narrowing of the visual field and a decrease or even the loss of vision in some retina areas.

The examination involves the assessment of the field of vision of one eye at a time: once one of the eyes is covered, the subject must stare at a central point in front of him/her where a visual stimulus is given. Then, she/he has to press a push-button when she/he perceives the stimulus. The test is then repeated for the other eye.

During the examination the instrument projects the stimuli according to an algorithm (called *strategy*) which aims to test the patient's light sensitivity threshold levels. At the end of the examination, the sensitivities measured in the various points of the retina are displayed in a graph, which highlights any possible areas of narrowing of the visual field.

The current limit of the instrument is represented by the duration of the examination: from 8 to 11 minutes. To overcome this limit, it is necessary to implement new projection algorithms

for new strategies, with same reliability as the current one but with shorter execution times. This is the aim of the present thesis.

In particular, this work is based on the creation of a simulator of healthy virtual patients and on the implementation of different strategies for the acquisition of the visual field. These are tested on the created virtual patients' model. In this way it is possible to evaluate the performance of the strategies without clinical trials that involve high time and cost.

In *Chapter 1* is introduced the anatomy and physiology of the eye, focusing attention on the pathology of glaucoma. The concept of the visual field for healthy patients is then introduced, comparing it with glaucoma patients.

In *Chapter 2* the perimetry is presented. The history and the development of the perimetric examination, the different types of perimetry and how the examination for the acquisition of the visual field is structured. The characteristics of different strategies are described, specifying positive and negative points for each one.

In *Chapter 3* is explained the thesis project. The COMPASS perimeter designed by CenterVue S.p.A. is described, the implementation of the various strategies taken into consideration for the project. The creation of a model of virtual patients on which to test the strategies and the simulation of the examination.

Finally, in *Chapter 4*, the results obtained are discussed. Initially, is explained the project by analysing the current status and the problems related to the perimetric examination for the diagnosis of eye diseases. Subsequently, the results obtained for all the strategies considered were compared. The model was tested to evaluate the performance of the algorithms applied to the virtual patients generated until establishing which strategy is a good compromise between all those considered in terms of error in estimating the threshold of sensitivity and number of projections (total acquisition time).

Abstract

The thesis examines the major problem of perimetric examination for the diagnosis and prevention of eye diseases such as glaucoma.

The typical subjectivity of the perimetric examination is caused by the duration of the diagnostic test and the validation of algorithms, called *strategies*, for the acquisition of the visual field of a patient. The aim of this work is to synthesize a simulator of virtual patients for COMPASS. Simulation allows to develop new strategies for the projection of light stimuli and to evaluate their performances compared to those of the algorithms currently used in clinical practice. Furthermore, it is important to simulate any software modification that impacts the instrument performance, before validating it in clinical field. This simulator will be used to develop and validate new strategies to reduce the examination time and to keep the measurement reliable. To this aim it generates thousands of virtual patients with specific reference characteristics (i.e. simulated field of view similar to healthy or pathological profiles).

In 2015, CenterVue developed COMPASS, a device for perimeter examination. This medical device is a fundus-automated-perimeter. It is different from traditional perimeters, as it acquires a photo of the retina at 25 Hz and uses it during the examination to correct any movements of the patient's eye in real-time (which would otherwise distort the estimate of the sensitivity map). At the end of the examination, the device provides the retinal sensitivity for all the tested points. This grid allows to estimate the patient's vision curve, that is, a vision hill with a central peak at the fovea and lower and lower values when moving away from the centre of the retina. The perimetric examination is the "gold standard" examination to highlight any defects in the field of vision due to glaucoma. The validation of strategies is possible thanks to different clinical, that are long and expensive. They require to recruit subjects who are willing to undergo the visual field examination several times and, in addition, there is no prior knowledge on their reliability. The examination of the visual field consists of projection of light stimuli at different intensities and retina positions in order to estimate a spatial map, named *grid*, of retinal sensitivity. During the examination, patients have to press a button every time they see a stimulus. The projection intensity sequence precisely detects the sensitivity threshold at one point. Each point of the grid is tested with a light intensity calculated using algorithms, called strategies, used to acquire the visual field. If a threshold is lower than a certain value, it corresponds to a pathology or blindness. The examination normally lasts from 8 to 12 minutes (depending on the presence or absence of pathologies) and it is stressful and highly variable for the patient.

1 Human Visual System (SVU)

1.1 Anatomy of the eye

The eye is considered the external organ of the visual apparatus, it consists of the eyeball and the eye attachments. It is able, through the light that is perceived, to process the external environment. When the light intensity is regulated by the diaphragm or iris, a specific lens system generates an image in the retina. This image is then converted into electrical signals transmitted to the brain via the optic nerve and processed for interpretation [1].

The eyeball is contained and protected in the orbital cavity, a pyramid-shaped bone structure. It consists of three concentric components: external component formed by sclera and cornea, the medium composed of choroid, ciliary and crystalline body, and finally the internal or nervous component formed by the retina [1]. The eye (ocular globe) has a spherical shape with a diameter of about 22-23 mm; while the spherical cap that deviates from the eyelids, called cornea, transparent and shiny, has a diameter of about 10 mm.

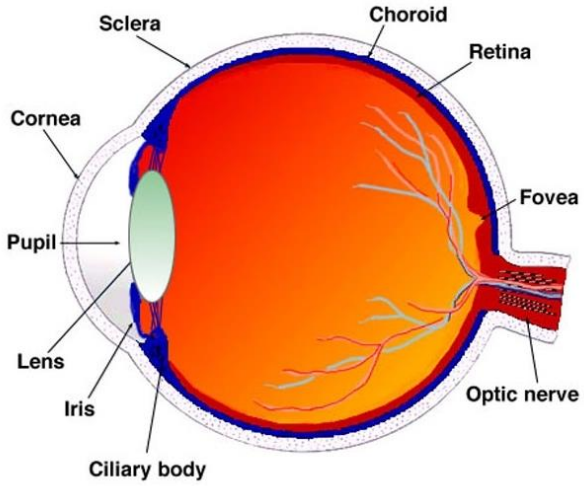

Figure 1.1: Near-axial (near-horizontal) section of the adult human eye. [4]

Moving towards the inside of the eye (Figure 1.1), near the cornea, is the iris: a ring of tissue whose colour varies from individual to individual. At the centre of the iris (Figure 1.1) there is the pupil, a black photosensitive hole penetrated by the light from the external environment. In the back of the pupil (Figure 1.1) is the biconvex lens shaped crystalline lens attached to a ring of muscle fibres named the ciliary body [1, 2].

The space between the crystalline lens and the cornea is filled with a gelatinous material called the humor vitreous.
Sclera, choroid and retina are the three layers that make up the part of the eye outside the cornea. The cornea is located in the anterior part of the sclera and has a fibrous tissue; the choroid shows a tissue rich in dark pigments (as well as capillaries) and finally the retina which is composed of photoreceptors called cones and rods, the light-sensitive elements (in detail in paragraph 1.2) [2].
Cones and rods are connected by thin fibres to other cells formed by two extensions: the bipolar cells. In the centre of the ocular globe there are ganglion cells, nerve cells consisting of ramifications, called dendrites, in contact with the bipolar cells and a fibre of discrete length that makes up the optic nerve [3].
The information acquired by photoreceptors is transmitted to the brain via the optic nerve, which is present at the exit of the eyeball through the papilla or optic disc (Figure 1.1), that is a blind area because it has no photoreceptors [3].
Analyzing the posterior part of the eye, there is a zone called macula (Figure 1.1) that inside presents the central fovea: a portion of the retina without rods but with a strong presence of cones characterized by a strong visual acuity [3].

1.2 The retina

Nervous tissue that almost completely covers the inner wall of the eye is the retina: a photo-transducer capable of picking up light signals and converting them into bioelectric signals. It is composed of photoreceptors (cones and rods), horizontal, bipolar, ganglionary and amacrine cells that participate in the first processing of the visual signal. Each of these cell types has a specific task and are organized in a layered structure [1].

The outer layer, called the pigmented epithelium, consists of a single layer of epithelial cells containing a dark-coloured pigment that impedes the diffusion of light by absorbing it. Continuing on, we find the photoreceptor layer: the cones and rods. Then we find the outer limiting membrane, outer granule layer, outer plexiform layer, inner granule layer, inner plexiform layer, multipolar cell layer, nerve fibre layer and finally the inner limiting membrane (Figure 1.2).

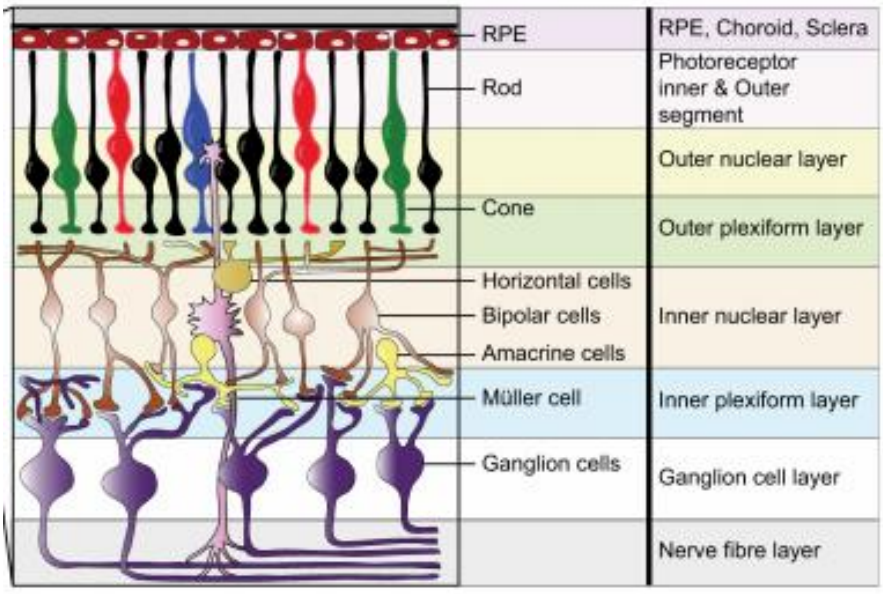

Figure 1.2: Detail of retinal cell structure: layered vision [5].

1.2.1 The photoreceptors: cones and rods

As already mentioned, photoreceptors play a key role in the visual system. There are about 120 million photoreceptors, median to night vision (scotopic vision), they are very sensitive to light and for this reason they are able to detect soft stimuli that the cones would not perceive.

The cones, about 6 million, are responsible for daytime vision, the functional loss of these cells is sufficient to be declared blind. There are 3 different types of cones, each containing a photopigment with sensitivity to a different portion of the electromagnetic spectrum. In detail, the photoreceptor structure can be divided into three main regions: the outer segment for phototransduction, the inner segment containing the cellular organelles and the synaptic segment where the information is sent to the bipolar cells (Figure 1.3). The cones are contained by disks contiguous to each other, as opposed to rods that become separate intracellular organelles [7].

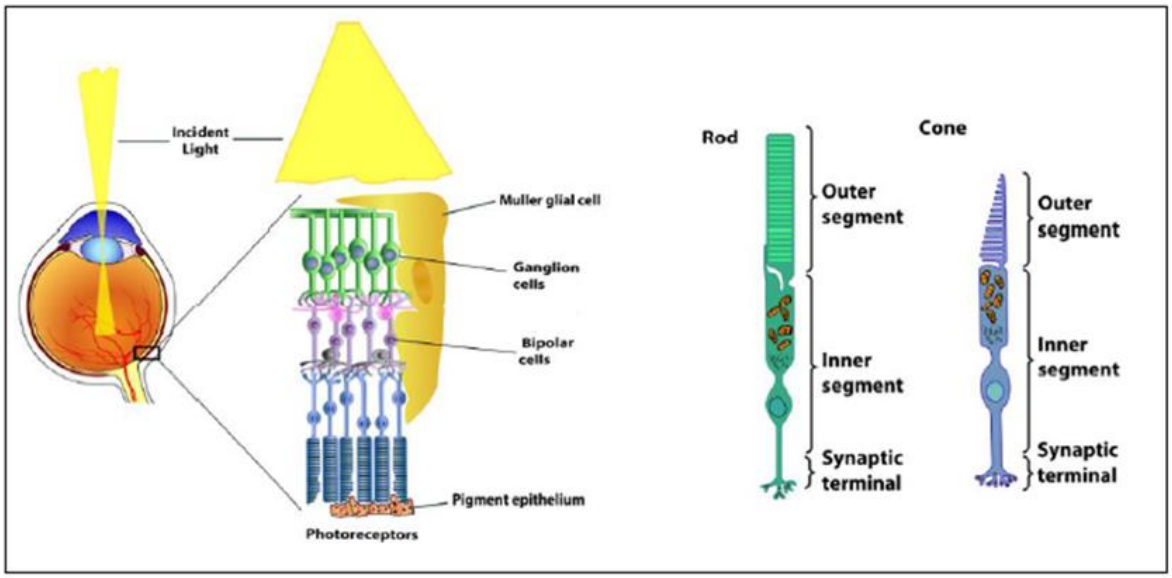

Figure 1.3: Anatomy of the retina and the structure in detail of cones and rods [6].

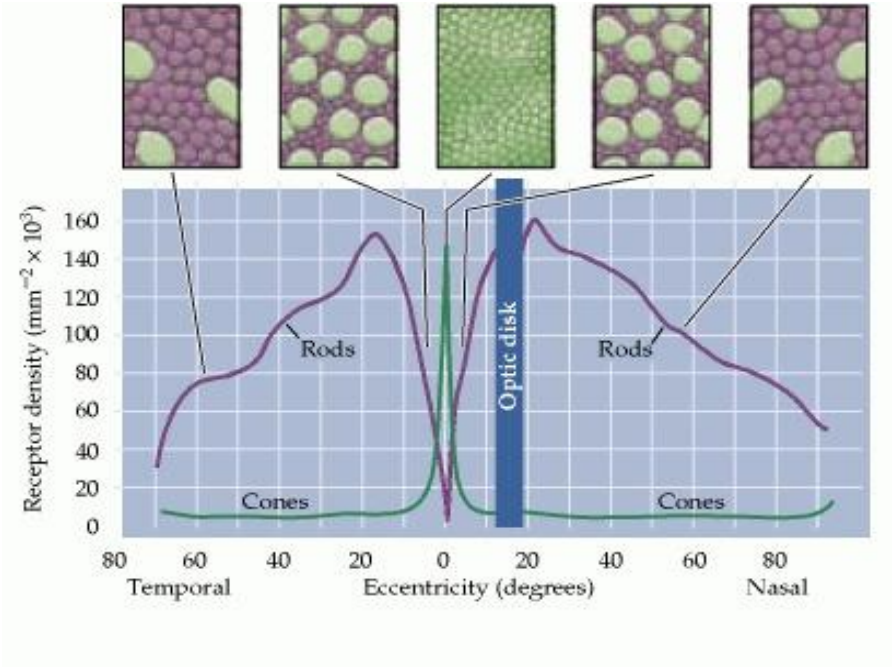

Figure 1.4: Distribution of rods and cones in the human retina. The graph shows that the cones are present at low density throughout the retina, with an acute peak in the centre of the fovea. In contrast, rods are present at high density throughout most of the retina, with a sharp drop in the fovea. The boxes above illustrate the appearance of cross-sections through the outer segments of photoreceptors with different eccentricities. The increase in the density of the cones in the fovea is accompanied by a significant reduction in the diameter of the outer segments [7].

The distribution in the retina of these photoreceptors (Figure 1.4) controls human vision. The density of the rods is higher than the cones. However, this relationship changes rapidly in the fovea (Figure 1.4) where the density of the cones increases almost 200 times, reaching in the centre, the highest density present in the retina [7].
This high density is achieved by decreasing the diameter of the outer segments of the cones so that the cones of the fovea resemble bars. The increase in the density of the cones in the fovea is accompanied by a marked decrease in the density of the bars. In fact, the central 300 μm of the fovea, called foveola, are totally without rods [7].

1.3 Retinal image formation

The complex process of forming an image in the eye is very similar to the operation of the camera: iris and lens correspond to diaphragm and lens. The visual sensation begins when the light passing through the pupil is focused by the crystalline lens on the pigmented epithelium: the bottom layer of the retina. The lens system of the eye forms an image of the processed objects in the retina which is inverted and smaller in size [7].
Light from the external environment penetrates the eye through the cornea and is refracted by the lenses and the cornea itself. The shape of the lenses can vary according to the needs of the eye when it needs to focus something at a certain distance (accommodation).
The distance between the lens and the imaging region (the retina) is fixed and the required focal length is achieved by varying the shape of the lens. The ciliary muscles increase or decrease the thickness of the crystalline lens for focusing (variable focal length lens). The focal length of the crystalline lens at rest is 17 mm [7].
The intensity of the light is then perceived by the pupil, which changes its size according to the amount of light radiation: enlarging in low light conditions and shrinking in the opposite case. Subsequently, the light passes through the crystalline lens which changes shape to convey the light into the retina.
In the retina, photoreceptors (cones and rods) absorb the light radiation by sending electrical potentials through a series of enzymatic processes involving photopigments. The impulses received are processed by the brain and transformed into an image. This process is called phototransduction: it causes hyperpolarization in bipolar cells, which transfer the information from photoreceptors to ganglion cells. The information from the approximately 130 million photoreceptors in the retina is thus compressed into electrical signals that are transported by 1.2 million neurons (bipolar cells, amacrine cells, ganglion cells and horizontal cells), whose axons

form the optic nerve. This transmits visual information to the primary visual cortex, which processes the image in terms of orientation, margins, etc. [7].

1.4 Retina fibers distribution

The nerve fiber (Figure 1.5) through every point in the retina and towards the head of the optic nerve, or optic disc. The characteristics of the defects in the visual field are related to the course of the nerve fibers, as will be further investigated later.

Physiologically it is known that from the nasal region to the optic disc, the fibers take a radial course towards the nasal edge of the optic disc itself. The fibers, which from the nasal side of the fovea move towards the temporal margin of the optic nerve, assume a straight course while those originating above or below the horizontal meridian from the temporal side of the fovea, assume an arched course and then move respectively to the upper or lower pole of the optic nerve [11].

The fibers, originated from the temporal retina, assume an arched course to reach the upper or lower pole of the optic nerve by jumping the fovea. If one imagines dividing the visual field into two parts, thanks to an imaginary horizontal line on the temporal side, the fibers located in the upper part form an arc in the upper area of the fovea to reach the upper pole of the optic disc. Similarly, the fibers at the lower part take on an arched course and surround the lower part of the fovea to converge at the lower pole of the optical disc [11].

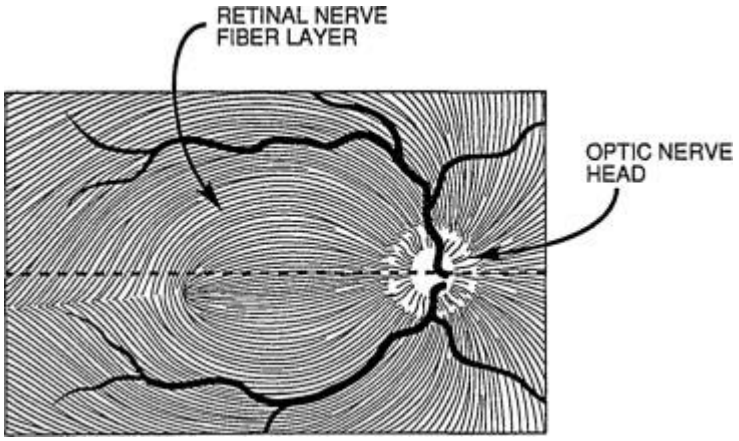

Figure 1.5: Distribution of retinal fibers [11].

Among all the numerous pathologies concerning the visual apparatus, attention will be focused on the pathology of glaucoma as it is closely related to the subject of the thesis.

1.5 The pathology of glaucoma

Glaucoma is a neurodegenerative condition affecting the eye and is associated with increased intraocular pressure (IOP) above 21 mmHg in the absence of morphological or functional damage to optic nerve fibers. If left untreated, patients with this condition may experience a loss of the visual field until complete blindness. Glaucoma can progressively cause neuropathy in the optic field and is characterized by structural changes in the optic nerve head or optic disc [9].

The diagnosis is made by ophthalmoscopy, gonioscopy, visual field examination, and measurement of central corneal thickness and intraocular pressure.

The safest way to recognize it is an accurate eye examination with the measurement of the endocular pressure, examination of the optical papilla and nerve fibres, and finally examination of the visual field [10].

The increase in ocular pressure due to an alteration in the outflow or the production of watery mood, if untreated, it can cause progressive and irreversible damage to the optic nerve over time (neuropathy glaucomatous) which results in damage to the retinal nerve fibres (Figure 1.6). Clinically with the loss of the visual field, which starting from its mid-peripheral portion, has a centripetal trend towards the macular area. It is because of this slow, progressive loss of the visual field that the patient realizes too late when the damage is advanced and no longer recoverable, that glaucoma is a serious and insidious disease. The damage to the visual field begins in the middle periphery and is often not felt by the patient who maintains a good central mink until the advanced stages of the disease [10].

Statistical forecasts show that glaucoma will be present in 80 million people in 2020 and more than 111 million in 2040. The prevalence of glaucoma is about 5-7% in the black population and about 3-5% in the white population of South Africa [10].

Open-angle glaucoma	Angle-closure glaucoma*
Accounts for at least 90% of all glaucoma cases	Is a less common form of glaucoma
It is caused by the slow clogging of the drainage canals, resulting in increased intraocular pressure	It develops very quickly
There is a wide and open angle between the iris and cornea	There is a closed or narrow angle between the iris and cornea
It involves symptoms and damage that are not readily noticed	It involves symptoms and damage that are usually very noticeable

Table 1.1: Differences between the two types of glaucoma.

Figure 1.6: From left to top: the loss of the upper portion of the visual field that progressively it gets worse by involving the lower area to leave only a visual residue.

1.5.1 Glaucoma Pathophysiology

The pathophysiology of glaucoma is not yet fully known but is related to the death of the ganglion cells of the retina. A better understanding of the pathophysiological mechanisms involved in the onset and progression of glaucomatous optic neuropathy is essential for the development of better treatment options. Normal physiological balance depends on the secretion of aqueous humor and its drainage. The aqueous humor is secreted by the ciliary body and the drainage of the humor takes place through two independent pathways: between the trabecular network and the scleral uveum outflow pathway. Filtration depends on pressure gradients, blood pressure and increased IOP [9]. Glaucoma can be classified as a primary hereditary disorder, secondary to a disease, trauma or medication, or as congenital in nature.

1.5.2 Glaucoma Typologies

There are different types of glaucoma (Table 1.1), such as open angle glaucoma and closed angle glaucoma. They are described in detail below.

1.5.2.1 "Open Angle" Glaucoma

Open-angle glaucoma can result from optic nerve damage with any degree of IOP. It is the most frequent type of glaucoma (90% of glaucomatous patients). The rate of progression can be fast or slow. Patients may experience an increase in IOP, and therefore only present with changes in the optic disc or visual field at a much later stage [9].

1.5.2.2 "Closed Angle" Glaucoma

Closed-angle glaucoma may be due to a physical blockage of the trabecular network. This may be more acute at the beginning than open-angle glaucoma. When IOP is > 40 mmHg, damage to the optic nerves and even permanent damage (> 60 mmHg) may occur [9].

1.5.3 Risk factors for glaucoma progression

Risk factors associated with glaucoma include: Pre-existing high IOPs, age progression, patients over 60 years of age are more likely to become glaucomatous. Other conditions such as diabetes mellitus, hypertension and hyperthyroidism contribute to its formation. In addition, eye cancers, retinal detachment, eye surgery, a family history of glaucoma (especially in young patients) contribute substantially to the onset of this disease [9].

1.6 The Visual Field in normal subjects

The visual field is defined as the area in which a person can see at a given time with respect to the direction of fixation, without head or eye movement (i.e. it defines the boundaries of the area beyond which nothing can be seen). The extension of the field of vision is an essential part of one's visual function, because a narrow field of vision has a significant negative impact on the activities of daily life and, consequently, on the quality of life [8].

The field of vision of only one eye is called the monocular field of vision (Figure 1.7). Its spatial extension in people with normal vision is limited by the person's facial anatomy, with the eye orbit, nose, forehead and cheekbones outlining the limits of the field of vision. On average, the monocular field of vision extends from 60° nasally to about 90° or more temporarily, and from about 60° above to 70° below. In persons with normal vision, the field of vision is binocular (Figure 1.8). This means that it contains input from both eyes, with integration and mapping of both eye information, allowing stereo acuity and depth perception. The visual information in the 60 central degrees of the visual field is processed by both eyes [8].

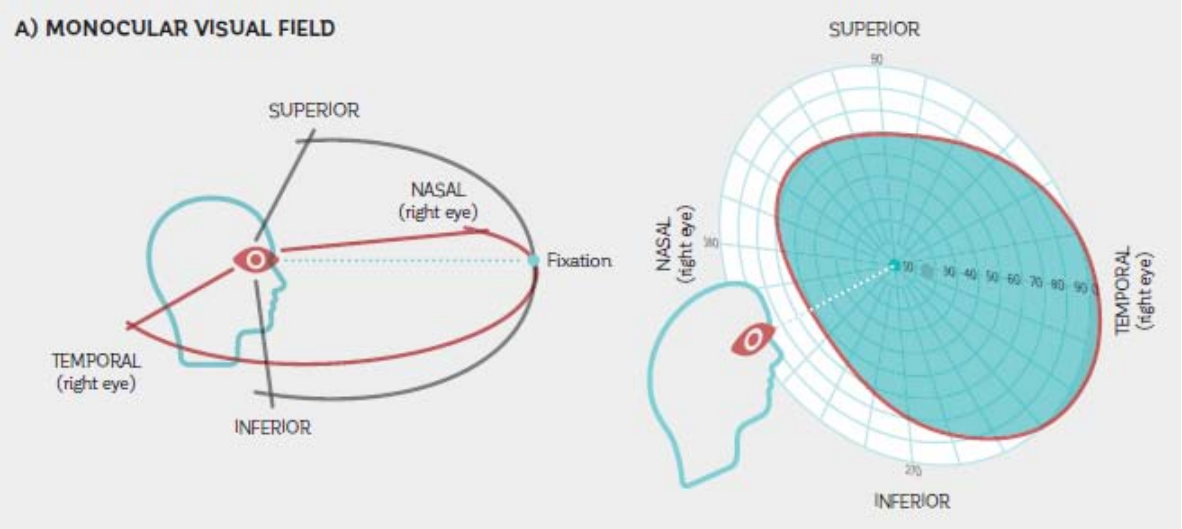

Figure 1.7: The monocular visual field of an eye is limited by the eye orbit, nose, forehead and cheekbones [8].

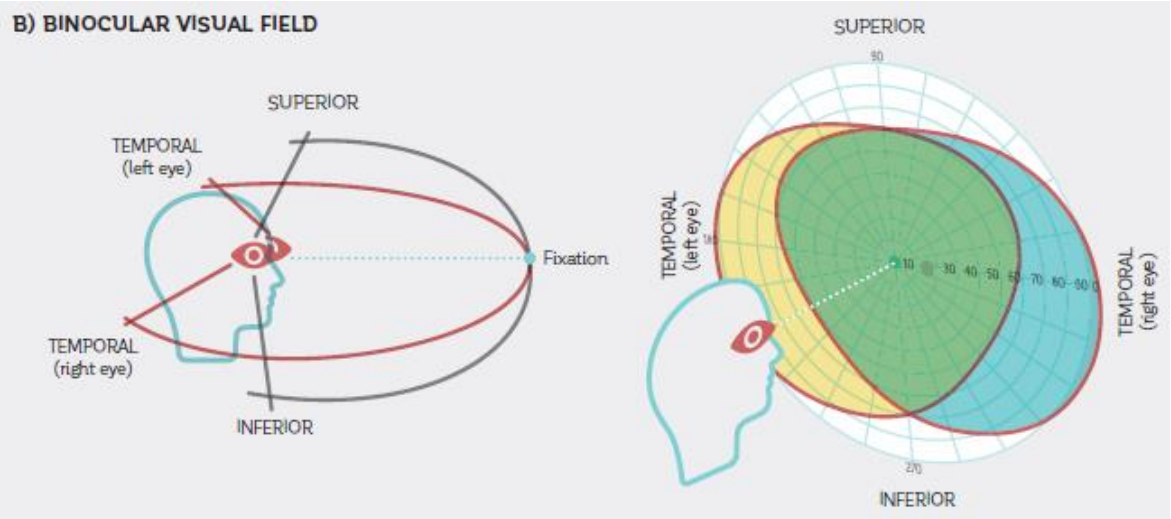

Figure 1.8: The binocular field of view of two eyes overlaps in the central area [8].

1.6.1 Light sensitivity in the field of vision

The area in which a person can see (extension of the field of vision) is not sufficient to describe a person's vision. It is also important to have a measure of sensitivity to light. The sensitivity of the eye is not constant throughout the whole field of vision but varies in a rather complicated way with eccentricity, level of adaptation and the nature of the test stimulus [8].

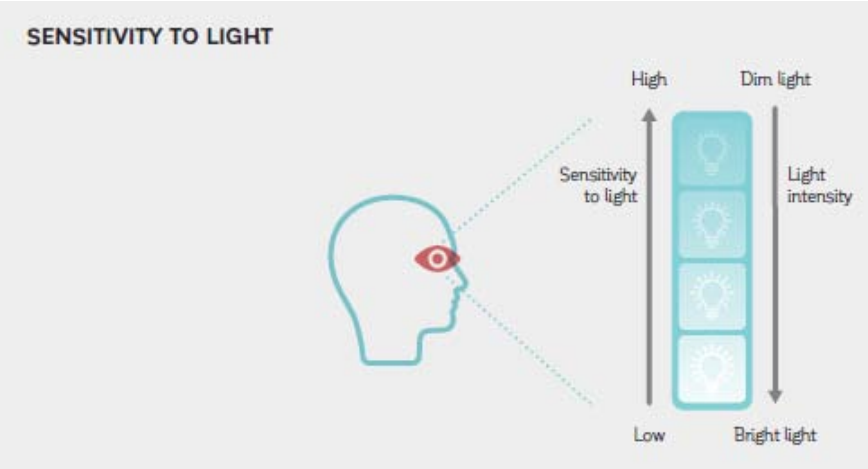

Figure 1.9: The figure illustrates the relationship between light intensity and light sensitivity. A person who can perceive very weak light has a very high sensitivity to light, while a person who can only perceive very bright light has a low sensitivity to light [8].

Light intensity and light sensitivity are inversely proportional: high light sensitivity corresponds to low light intensity and vice versa (Figure 1.9).

To represent the different sensitivities in different regions, the field of vision is described as "an island of vision in a sea of darkness". The height or elevation of the island represents the sensitivity of the eye. The stimuli whose parameters place them above the island are too weak to be seen [8].

1.6.2 Hill of Vision

The sensitivity of the eye is not constant throughout the entire field of vision indeed it varies with eccentricity, adaptation level and the nature to the test stimulus. Because of the representation of different regions, the visual field is defined like an "island". Tarquair describes the visual field as an "island of vision in a sea of darkness" (Figure 1.10). The sensitivity of the eye is the height of the island: the intensity of stimuli above the island are too weak to be seen, while those who fall into the "sea" are out of sight and cannot be seen regardless of their intensity (in not possible to see them no matter how bright they are) [1].

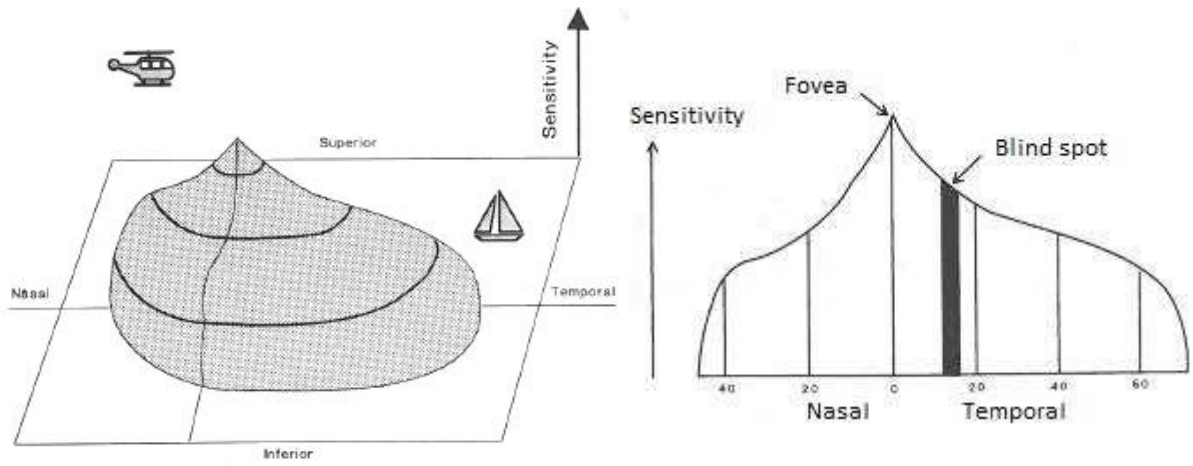

Figure 1.10: Left, mink island or hill of vision.

The four portions of the visual field (Nasal, Temporal, Upper and Lower) are highlighted, and retinal sensitivity (or sensitivity) is the amount that determines the height of the hill. On the right, section of a vision island; the high peak is in correspondence of the fovea while the portion in which the retina presents the optical disc is blackened. This point is called a blind spot or blind spot [1].

The vision curve (or HoV "Hill of Vision") is therefore a three-dimensional representation of the sensitivity of the retina. The value of the average sensitivity at each point of the visual field, which is represented by the viewing curve, may be representative of a certain population. It is defined as the average sensitivity found in a normal population within a certain age range, for a certain point in the test. The curve decreases annually by a certain amount (about 0.065 dB per year) starting at the age of 20 [1].
The hill of vision depends on the light: when the eye is accustomed to the darkness, the vision curve is higher and more sensitive and due to the distribution of cones and rods it has a crater in the centre: the crater of the fovea (Figure 1.11); while when the eye adapted to the light (photopic vision) the vision curve is at low altitude and has the centre corresponding to the fovea [10].

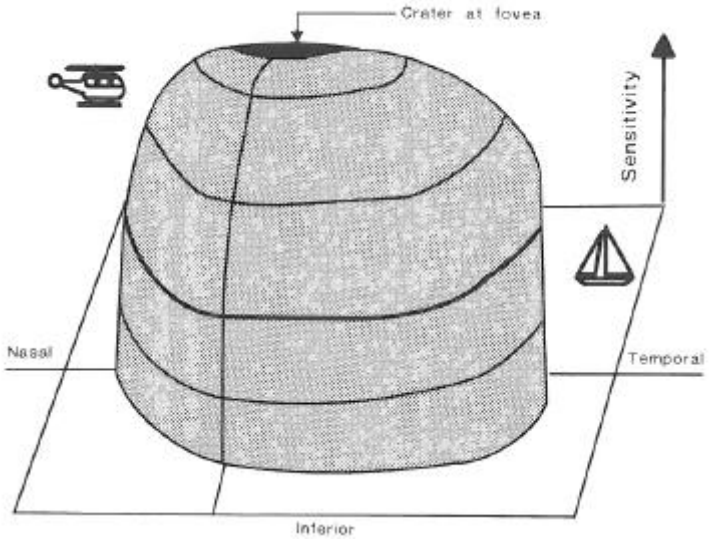

Figure 1.11: Hill of vision for dark-adapted eye [1].

1.7 Visual Field in glaucomatous subjects

The glaucoma, a pathology that can cause damage to the visual field, is in clinical practice the most common reason for requiring a perimeter examination [12].

In glaucoma, the axons of the optic nerve are damaged, therefore visual function is diminished or lost in the retinal area innervated by the damaged axons. The most frequent damage is the one that affects one or more bundles of nerve fibres that innervate a particular region of the retina. In these cases, the visual sensitivity may initially be reduced only in some points, and then extend to other non-contiguous regions, while others retain normal sensitivity [13].

During the progression of this disease, all the regions of the field visual are involved and eventually the eye totally loses its visual abilities. The speed at which certain points or the entire visual field is damaged is variable. At first, the damaged regions show a reduction in sensitivity, until no perimetric stimuli can be perceived, while other regions remain normal [13].

Perimetry (described in Chapter 2) still remains the gold standard in the detection of loss of field of vision, and in monitoring its progression. Two are the fundamental aims of the perimeter: the screening (identifying whether or not there are defects in a patient's field of vision) and follow-up (the evaluating the progression of a defect highlighted in an examination). The aim of the treatment of glaucoma is to safeguard visual function, by means of therapies pertinent. Thus, it is important to differentiate patients with progressive vision loss slowly, compared to patients whose glaucoma is more aggressive. The set of tests of the same patient over the course of the months, allow the doctor to estimate the rate at which visual function will deteriorate, in order to intervene in the most appropriate way [12,13].

It is more useful to identify a glaucoma in the pre-perimetric phase, but the field of view has no defects, so you can intervene in a timely manner. The variety of localization of glaucomatous perimetric defects and the rarity of a uniform and widespread involvement, have important diagnostic consequences. The discovery of a localized defect of moderate degree is possible for the threshold sensitivity values. In the various localizations are compared not only with the range of normal values, but also with the sensitivity threshold of contiguous points and other locations of the field of vision. A moderate but inconstant deviation of the sensitivity threshold values is recognized as pathological with more certainty than a fairly constant deviation from the normal values [12].

The generalized defect requires more axons of the optic nerve to be damaged than the localized defect, so that there is a visible reduction in the threshold. Many defects localized can only be recognized when a significant percentage of nerve fibers are destroyed, but less than the one destroyed in the case of a generalized defect. The pattern of defects helps to reduce the possible diagnosis of glaucoma. There are in fact typical features such as scotoma that help to immediately identify glaucoma [12].

The characteristics of defects that arise in the visual field are intrinsically linked to the physiology of retinal fibers. They pass through every point of the retina, and head towards the head of the optic nerve. In glaucoma, the nerve fibre bundles are damaged at the optic disc and the region of the visual field. innervated by these fibers loses its visual sensitivity. The result is a scotoma or depression located. Usually the first glaucoma damage is evident in the upper or lower arched beam. For this reason, according to the now classic descriptions, the perimetric defects of glaucomatous can be represented by a paracentral scotoma. The latter is an indication of damage to the arched beam in the so-called Bjerrum region5, characterised by a depression in the nasal part of the visual field, or from both of them [1,12,13].

1.7.1 Features of glaucomatous visual field defects

More commonly the visual field loss is an isolated defect. The glaucoma visual field appear to be fairly non-specific although the typical loss depends on the axons of the retinal ganglion cells in the retinal fibers. Relatively specific glaucomatous visual field defects include (Figure 1.11) [12]:

- Nasal step defect obeying the horizontal meridian;
- Temporal wedge defect;
- Classic arcuate defect (comma-shaped extension of the blind spot);
- Paracentral defect 10–20º from the blind spot;
- Arcuate defect with peripheral breakthrough;
- Generalised constriction (tunnel vision);
- Temporal-sparing severe visual field loss
- Total loss of field.

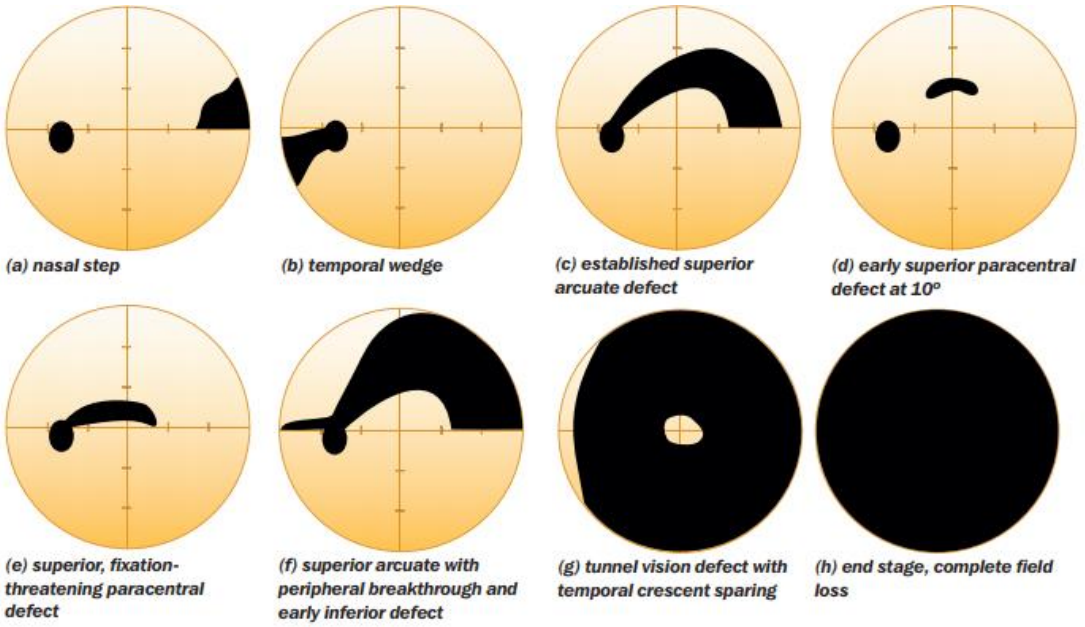

Figure 1.12: Scheme of glaucomatous defects in the left eyes [12].

Typical glaucomatous field of vision defects can be divided according to the characteristics and the area in which they appear. In detail, therefore, they are discussed below. Starting from the left you can see a grid of values of retinal sensitivity thresholds, its representation in grayscale and two maps indicating the anomalous zones based on the deviation from the population of the normal [23].

Typical glaucomatous field of vision defects can be divided according to the characteristics and the area in which they appear. In detail, therefore, they are discussed below. Starting from the left you can see a grid of values of retinal sensitivity thresholds, its representation in grayscale and two maps indicating the anomalous zones based on the deviation from the population of the normal [23].

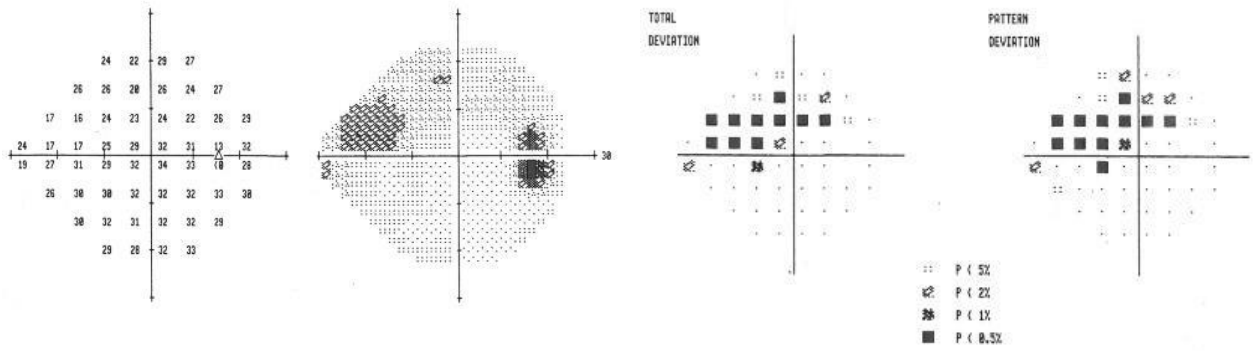

Figure 1.12: Large relative upper arch-shaped scotoma [23].

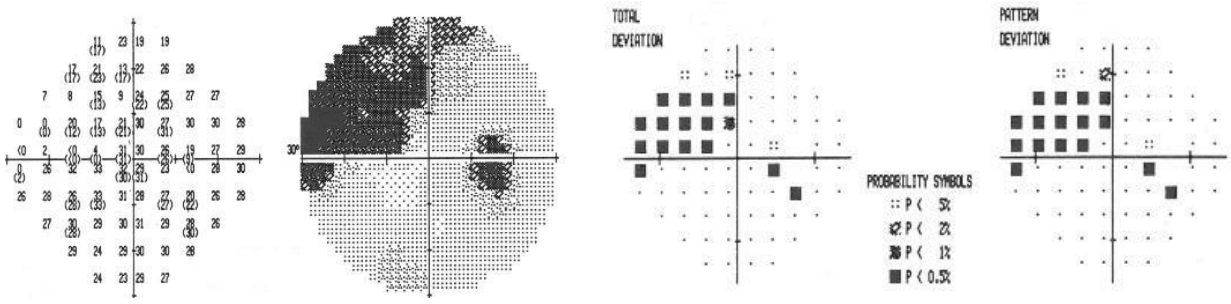

Figure 1.13: Depression of superior nasal sector [23].

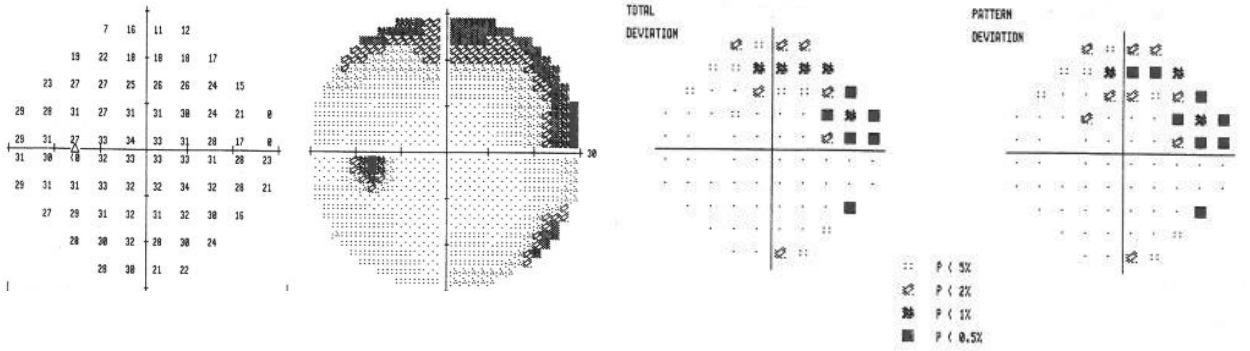

Figure 1.14: Early glaucomatous defect in the upper nasal area of the visual field [23].

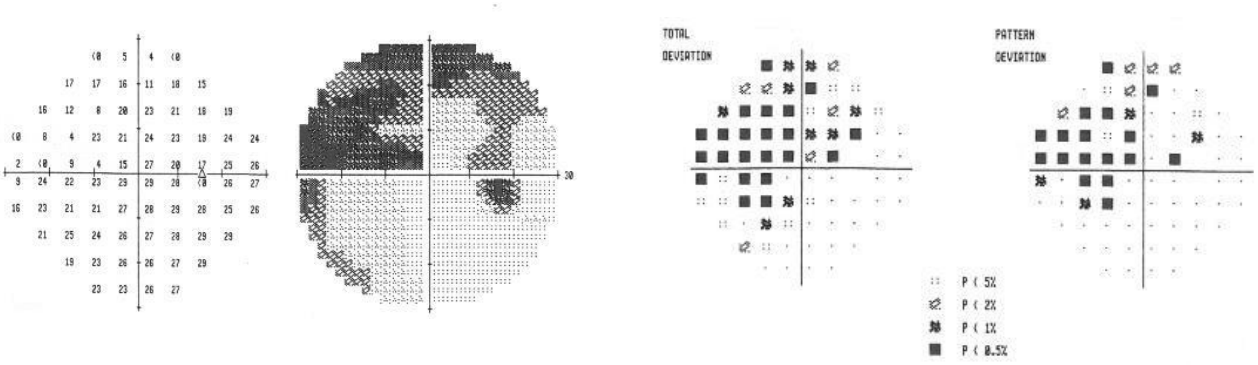

Figure 1.15: Upper nasal depression with threat of fixation point involvement [23].

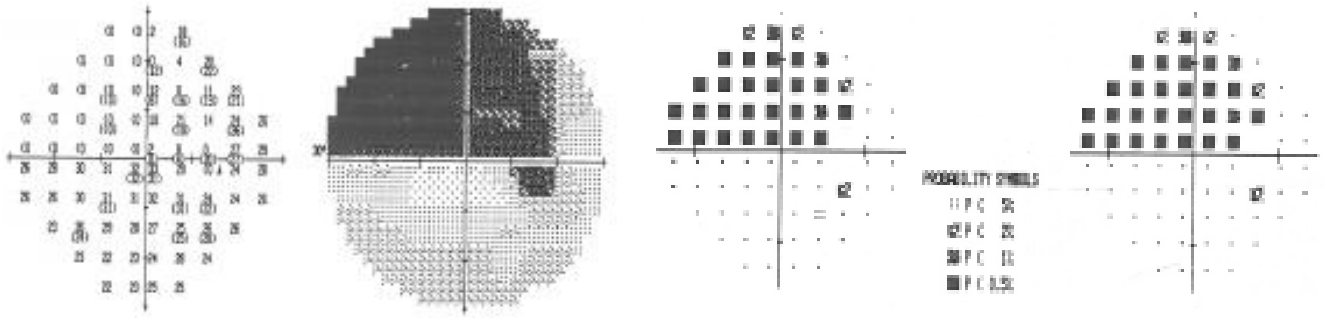

Figure 1.16: Absolute defect, whose arched shape is still evident [23].

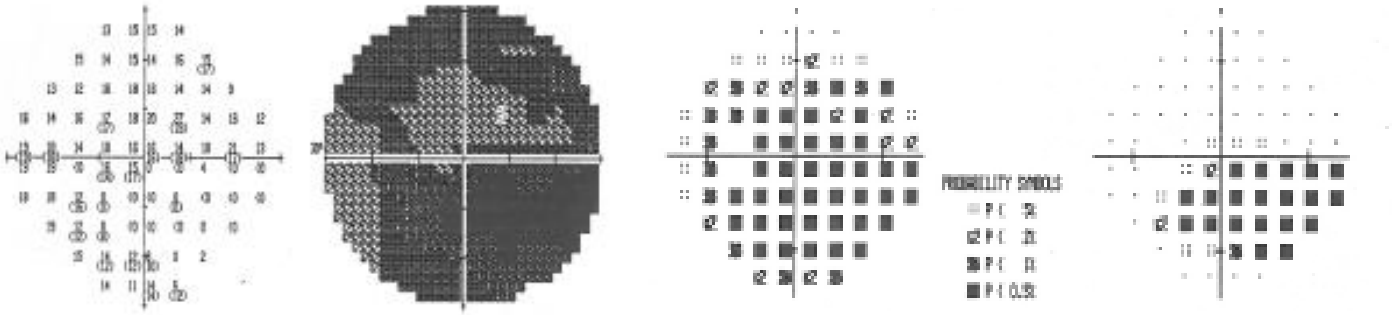

Figure 1.17: More advanced glaucoma [23].

COMPASS, a fundus automatic perimetry produced by CenterVue S.p.A, is the medical device on which we focused for this particular project and is used for the diagnosis of glaucoma.

1.8 Fundus Image

The fundus image is very useful for the diagnosis of glaucoma as it causes visible structural changes to the optic nerve. The acquired image of the retina is called fundus image and is used by the clinician to highlight any alterations or deformations. For the diagnosis of glaucoma, the perimetric examination is not sufficient and therefore the fundus image is necessary (Compass at the end of the perimetric examination also provides the retinal image to help the doctor with the diagnosis).

The following features are considered for diagnosis in ONH (Optic Nerve Head). The changes that characterize the presence of glaucoma in the ONH (optic nerve head) region: enlargement of the excavation, increased cup/disc ratio, disc haemorrhages, neuroretina edge thinning, cup asymmetry between right and left eye, loss of retinal nerve fibres and occurrence of parapapillary atrophy. Compass is able to acquire colour and infrared fundus images, which are then superimposed on the sensitivity grid in order to create an immediate correspondence between the points of the grid and the patient's retina.

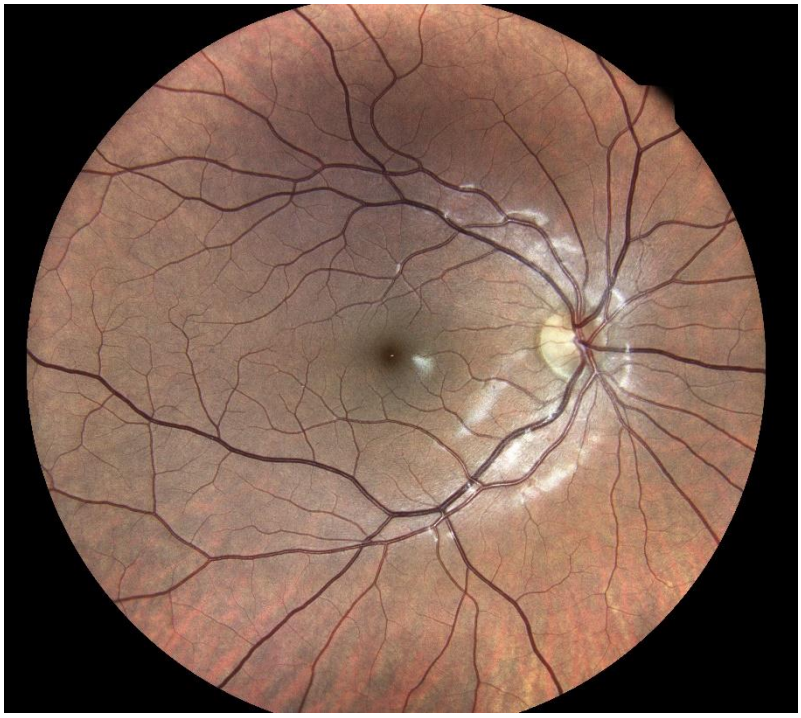

Figure 1.18: Fundus images.

2 Perimetry

2.1 History of perimetry

Through perimetry, a medical diagnosis, it is possible to test the field of vision: with "test targets" projected on a background, the sensitivity to light of the field of vision is determined. The term "perimetry" derives from the fact that it consists of mapping and quantification of the field of vision, especially at the extremes of its perimeter. This examination is generally performed by asking the patient to look at a fixed point, presenting objects at various points within his field of vision [15].

One of the first experts in perimetry was Hippocrates towards the end of the 5th century B.C. Later, Ptolemius in 150 B.C. tried to quantify the field of vision by deducing that its shape was approximately circular [16].

It is due to T. Young the first measurement of the visual field, which took place at the dawn of the 19th century, reported the size of the normal human visual field: upper radius 50°, lower radius 70°, nasal radius of 60° and temporal radius of 90°. Only in 1700 were described by Boerhaave the scotomas: areas of the visual field that correspond to blind parts [17].

Everything concerning the measurement of the visual field before 1800 is considered qualitative, since only in 1856 was published an article entitled "*Examination of the visual functions in amblyopic affections*" by Graefe, who is considered one of the most important figures who introduced the perimetry and the visual field test in clinical ophthalmology. In fact, the article introduces examples of loss of visual field, indicated as amblyopic affections because at the time the association of high intraocular pressure, cupping of the optical disc and loss of visual field was not fully integrated in an operational definition of glaucoma [18].

2.2 What is perimetry?

Perimetry is a systematic measurement of different light sensitivity in a visual field. It is used in ophthalmology for diagnostics, for example for glaucoma.

Objects/stimulus are presented in different areas of the field of vision while the patient's gaze remains fixed at a certain point. In this way it is possible to test the functional capacity considering the weakest object/stimulus perceived by the subject under examination (Figure 2.1) [19].

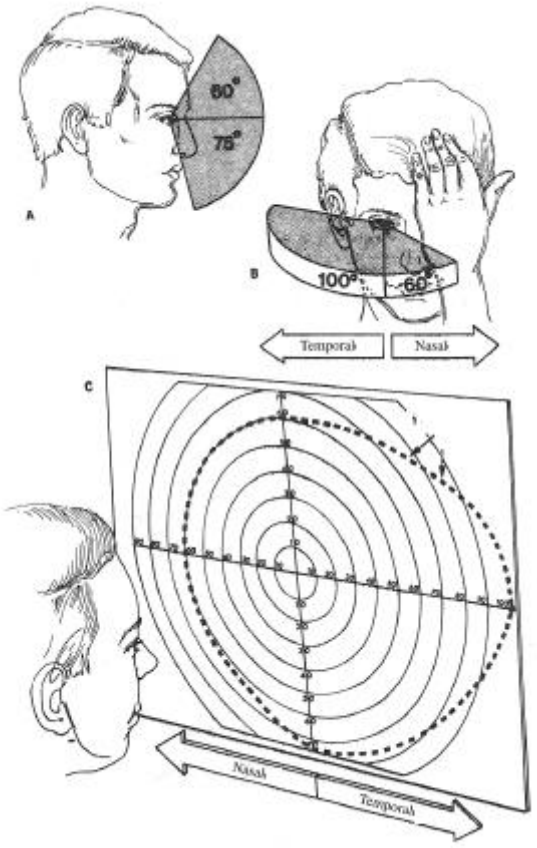

Figure 2.1: a) Superior and inferior visual field. b) Temporal and Nasal visual field. c) Visual Field limits [23].

The perimetry exam aimed to detect anomalies in the visual field: it was once carried out manually by an operator, who moved objects within the patient's visual field, while the latter kept his gaze fixed on a point in front of him. If the object was not perceived at the operator's request for confirmation, an anomaly in the field of vision was identified. By the time, tools were introduced that allowed the projection of luminous stimuli, until they were completely computerized [19].

During the perimetric examination, the differential sensitivity in various points of the retina is determined following the projection of a light stimulus on a background also illuminated. This is done in different points of the retina, according to predefined grids, and under standard test conditions, so that deviations from normal values can be identified. In order to allow comparisons between the data obtained in various examinations, it is necessary that the conditions under which the test is carried out, (i.e. stimulus size, background light intensity, stimulus exposure time and stimulus colour) remain unchanged [20].

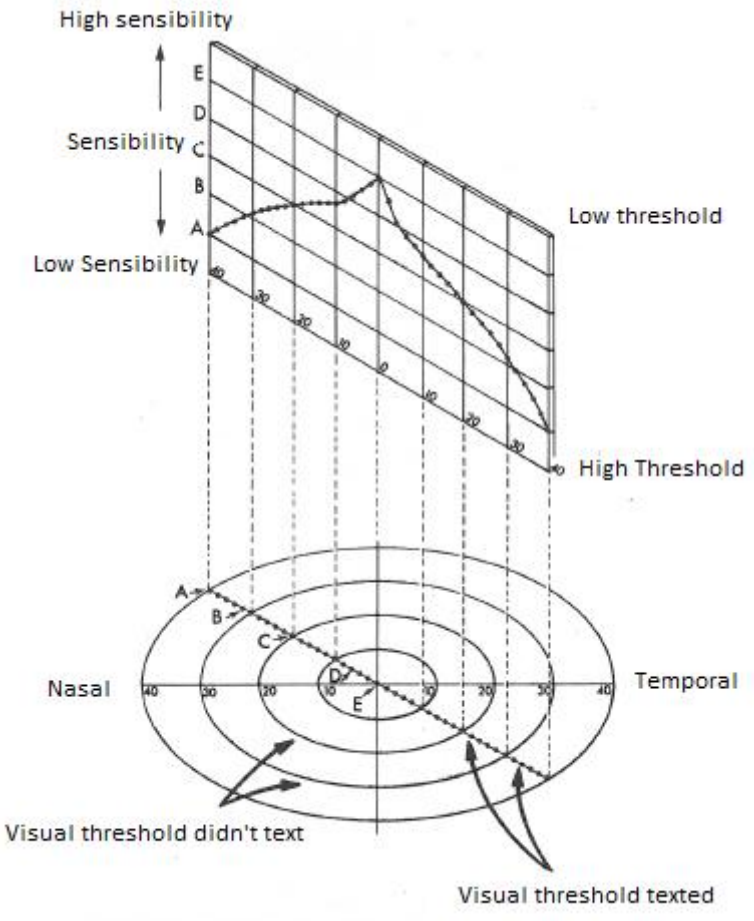

Figure 2.2: Perimetry is performed in the upper nasal quadrant, through the fixation point, to the lower temporal quadrant. The points where the threshold was examined are A, B, C, D, E. The image shows that at the point of fixation the sensitivity is maximum. This statistical scheme is not used in the clinic but is however considered to express the concept of greater visual sensitivity at the centre [23].

The differences in height between the normal vision curve and that of a depressed field of view correspond to local losses of retinal sensitivity (Figure 2.2). The values determined by the perimeter are the visual thresholds. The threshold of a patient in a certain point on the

retina is defined as the luminance of the stimulus, which is perceived with a 50% probability as described by the FoS (Frequency-of-Seeing curves).
In clinical practice the values of the thresholds are not expressed in physical luminance values (asb or cd/m) but in decibels (dB) [19, 20].
The limits of the field of vision, measured in degrees from the point of fixation (point at which the gaze is directed), are the following: 60° above, 70-75° below, 90-100° temporally, and 60° approximately nasally. The absolute limits of the field of view can be determined by carrying out a large object from behind the head of an individual who is looking straight ahead and asking him/her to report the object as soon as you become visible. If a pathology has resulted in a narrowing of the peripheral limits of the field visual, it may be necessary to move the object a lot for it to be perceived.
Perimetry is assessed through a hemispherical surface into which the visual field is projected. The examined eye is positioned in the geometric centre of the hemisphere, so all points are equidistant from the eye [19].
There are different types of perimetry: tangent screen, Goldmann perimeter, automated perimeter and micro perimeter.

2.3 Perimetry Types

As mentioned before, there are different types of perimetry that are used to detect visual field or for medical diagnosis.

2.3.1 Tangent Screen Perimetry

The simplest form of perimetry uses a white tangent screen. Visual capability is tested with the presentation of points (sights) of different sizes connected to a black stick, which can be moved, against a black background. This stimulus test (mire) can be white or coloured [20].

2.3.2 Goldmann Perimetry

The Goldmann perimeter is a white spherical cap positioned at a certain distance in front of the patient (Figure 2.3). An examiner presents the patient with a test light of variable size and intensity. The light can move towards the centre from the perimeter (kinetic perimeter), or it can remain in a certain position (static perimeter). Goldmann's method is capable of testing the full range of peripheral vision and has been used for years to track vision changes in glaucoma patients. However, nowadays, the examination has been supplanted by automated perimetry [20].

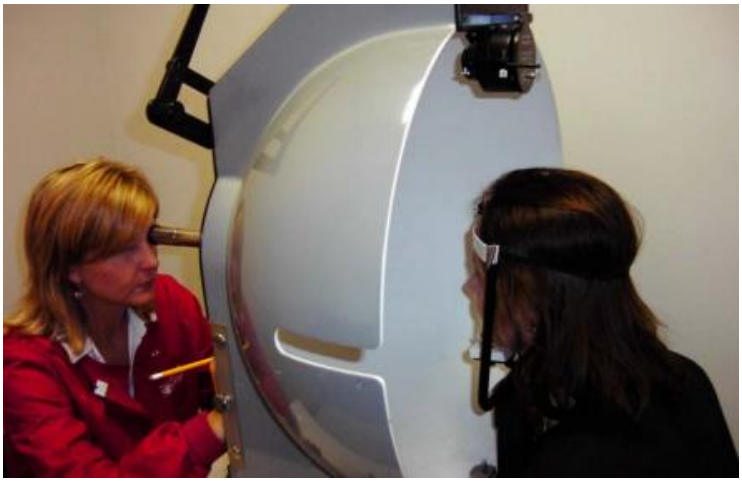

Figure 2.3: Positioning of examiner and patient for Goldmann Perimetry

2.3.3 Automated Perimetry

Automated perimetry uses a cellular stimulus moved by a perimetry machine. The patient indicates whether they see the light at the push of a button. The use of a white background and increasing brightness lights make this perimeter also referred to as "white on white". This type of perimetry is most commonly used in clinical practice and research studies where loss of field of view must be measured. However, the sensitivity of white on black perimetry is quite low, and the variability is relatively high. According to some studies it is possible that about 25-50 % of photosensitive ganglionic retinal cells may be lost before changes in visual field acuity are detected.[20]

2.3.4 Microperimetry

The microperimeter evaluates the macular function in a computerized way. In some experimental studies, a significant improvement in visual acuity, retinal sensitivity fixation behaviour and reading rate was found in treating senile macular degeneration or myopic macular degeneration with biofeedback treatment (Figure 2.4).

Figure 2.4: MAIA, an example of microperimetry device produced in CenterVue SPA, represents the latest advance in confocal microperimetry. Retinal images are acquired by Scanning Laser Ophthalmoscopy (SLO). An eye tracker allows accurate, real-time, compensation of eye movements. Luminance levels are compliant with existing standards (1000 asb.).

2.4 Threshold measurement: how to present the stimulus

The modality of how the stimulus is presented can be divided into two macro-sectors: static perimeter and dynamic perimeter.

In detail, static perimetry tests different areas of the entire field of view one at a time.

At first, a dim light is presented to the patient in a particular position. If the patient does not see the light, it is increased in intensity until it is perceived. The minimum brightness required to detect a light stimulus is called the "threshold" sensitivity level for that specific position. This procedure is then repeated several points until the entire visual field is tested. The threshold sensitivity level during static perimeter is generally tested using automated instruments. This type of perimetry is typically used for rapid screening and follow-up of diseases involving deficits such as scotoma, peripheral vision loss, and loss of central and clear vision [23].

Kinetic perimetry uses a cellular stimulus moved by an examiner (the perimetrist).

This is what happens, for example, in Goldmann's kinetic perimetry. Only one test light of constant size and brightness is used in the initial phase of the test. The test lamp is moved from the periphery to the central viewing areas until it is detected by the patient. This manoeuvre is repeated by approaching the centre of vision from different directions. Repeating this manoeuvre numerous times will establish a vision limit for that target.

The procedure is repeated using several test lights that are larger or brighter than the test light initially tested. In this way the kinetic perimeter is very useful when mapping the field of view sensitivity boundaries. This test can also be a good alternative for patients who have difficulty with automated perimetry, i.e. because they are unable to maintain a constant gaze or have cognitive impairment [23].

One way of representing the field of view, which is the output of the perimeters used in the clinic, is through the use of a diagram or grid (Figure 2.5).

This grid shows, point by point, the sensitivity of the visual field corresponding to the different points on the retina [23].

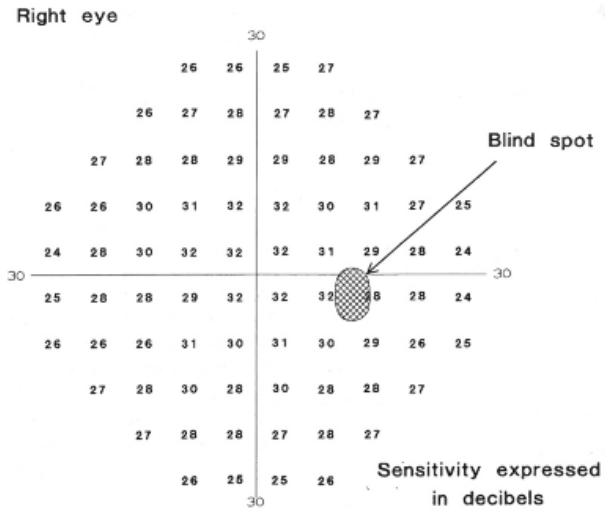

Figure 2.5: Sensitivity map in different points of the retina.

Therefore, after having tested the sensitivity threshold of a subject, it is shown schematically in a grid of predefined points (the most used one is 24-2 with 54 points) expressed in dB [22, 23]. Each point in the retina corresponds to a point in the visual field: for example, the fovea corresponds to the fixation point. The fovea is located in the centre of the macula, corresponds to the circular portion of the visual field, with a radius of 10°: this area of the retina allows a refined vision of details and a distinction of colours. This is the reason why this area has a much higher sensitivity than the peripheral region in the detection of light stimuli during the examination of the visual field. The points located in the peripheral part of the retina, near the ciliary bodies, correspond instead to the peripheral points of the visual field [23].

Moreover, since the image formed by the optics of the eye is upside down and overturned, as in a camera, in order to superimpose an image of the retina on the visual field, it is necessary to overturn the upper-bottom and right-left part. The nasal retina is therefore responsible for the vision of objects that are in the temporal field of vision and vice versa, the temporal retina for the vision of objects that are in the nasal field of vision. In addition, the points of the upper part of the retina allow the vision of the lower part of the visual field, and vice versa the lower part of the retina the vision of the upper part of the visual field [23].

The visual information acquired by all points of the retina is, as mentioned above, converted into nerve impulses which are carried by the fibres on the surface of the retina, and which converge at a point about 10-15° from the fovea in the nasal hemicampus, called the blind spot (Figure 2.6).

The fibers converge to form the optic nerve, which then reaches the brain: the point where the nerve fibers join together to form the optic nerve is called the optic disc. In order to allow the fibers to escape, a hole in the retina is inevitable, and therefore in this region of the visual field called "blind spot" (blind spot or physiological blind spot), stimuli are not perceived (Figure 2.6). Since the optic nerve is located in the nasal area of the eye, the blind spot will necessarily be located in the temporal portion of the visual field, in an area 10-15° from the point of fixation.

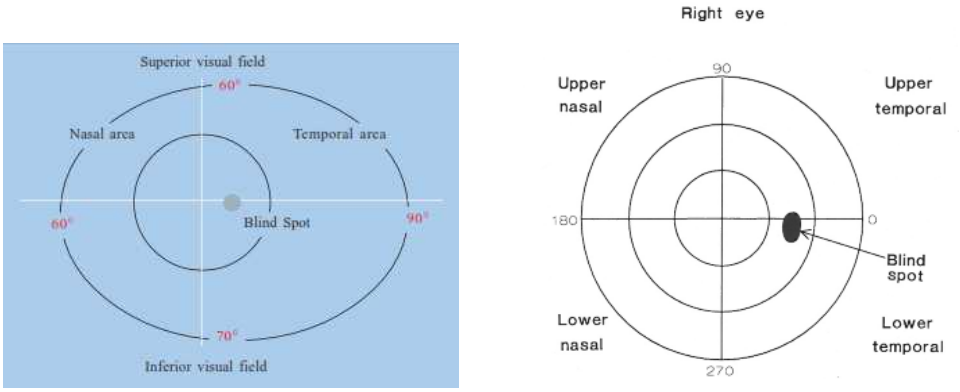

Figure 2.6: Field of vision limits in its representation. On the left realistic representation; on the right field of view in the representation used by the perimeters.

2.5 Algorithms for threshold evaluation in automated perimetry

Many medical devices for visual field acquisition have algorithms to determine the sensitivity at each point during the test: the most common are the full-threshold method, SITA standard, SITA Fast and ZEST. These algorithms are called strategies.

Each strategy can be used on a 30° pattern or even one that covers the 24° centers of the visual field (Figure 2.7). The strategy chosen the number of wise points affect the duration of the test. Threshold tests are used to determine threshold sensitivity. The tests determine whether the visual sensitivity at a given point is better than a selection criterion. Such a test can result in an abnormality but does not quantify its depth of the damage. It has the advantage of speed if only one stimulus is present. It is mainly used for the detection of defects (screening), for the topographic characterization of an anomaly (diagnosis), to quantify the limits of the visual field.

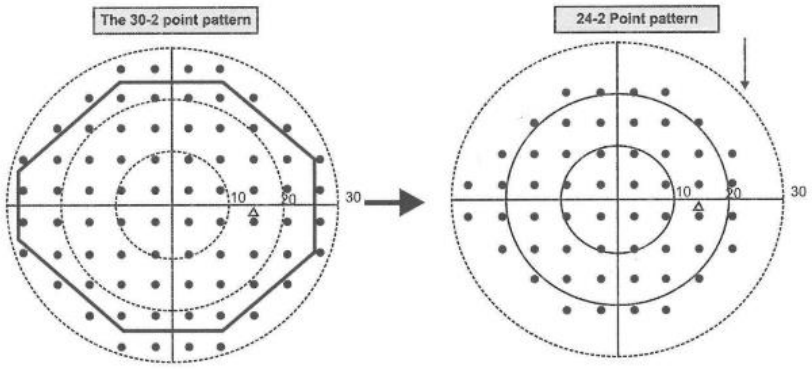

Figure 2.7: The number before the hyphen (30 or 24) indicates the area of the field examined, in degrees of fixation. The 24° strategy examines 54 points while the 30° strategy examines 76 points. The two grids of points that are tested during the perimetric examination are shown.

2.5.1 Full Threshold Strategies

The duration of the examination obviously depends on the number of points being tested, the strategy used, and by the patient's reaction time. Although the accuracy of the results is greater when using the strategies based on the standard grid and full threshold, when the duration of the test becomes too long, the "fatigue" effect plays a negative role. It is therefore good to look for a compromise between speed and accuracy [23].

The method for determining sensitivity is called "test strategy", and there are currently various strategies. The traditional strategy is called full threshold algorithm strategy. This algorithm provides for measure the threshold sensitivity at each point, using a procedure called "staircasing" or "bracketing" [23].

The brightness of the stimulus is made to vary (increasing or decreasing) by following steps, from whose name is "staircasing."

Varying the brightness of the stimulus in appropriate steps, the patient's threshold at each point is found, i.e. the brightness value that is perceived by the patient with a 50% probability. The stimulus projection program presents the patient with a series of more or less bright stimuli at all points on the grid to be tested, in random order. At the same time, the answers (Seen or Not seen) given by the patient. At each point to be tested, the intensity of the presented stimulus is slightly greater than the sensitivity that the patient is expected to have at that point and this value is derived based on the thresholds of nearby points. Each time the stimulus is seen, the patient presses the button, and the next stimulus that will be presented at the same point will be 4 dB less bright (4 dB higher in the sensitivity dB scale). This is repeated until the stimulus is too little intense to be seen. At this point the intensity is increased again in 2 dB steps until the following is seen again. Finally, if the strategy is 4-2 the intensity of the last seen stimulus is the threshold value in that point, if the strategy is 4-2-1 an adjustment of 1 dB is made in the opposite direction to the of the last step of 2 dB and the threshold is determined. If the stimulus projected at the beginning is not seen, the process is reversed: the stimulus is re-presented by increasing its intensity with steps of 4 dB up to when it is seen; from this point on, its intensity decreases with steps of 2 dB, until is not seen. The last value seen is the threshold. In the case of 4-2-1 the adjustment of 1 dB in direction opposite the direction of the previous steps by 2 dB [23].

The strategy begins by testing four primary points, each of which is in the centre of a quadrant of the field of view. These points are tested with a light intensity 4 dB lower (brighter stimulus) than the normal value corrected for age, followed by a decrease of 6 dB in the brightness of the stimulus (increase in intensity) when the patient does not respond to the first stimulus. The procedure continues by increasing the intensity of the stimulus with steps of 8 dB, to reach and cross the threshold: at this point the patient says he has seen. After this first crossing of the threshold, the staircase procedure decreases the light intensity of the stimulus by 4 dB. After a not seen (second threshold crossing), the stimulus intensity is increased with 2 dB steps (third crossing). Finally, an adjustment of 1 dB is made in the opposite direction to the last step of 2 dB to obtain sensitivity with +/- 1 dB accuracy. After determining the threshold at the four points, one for each quadrant, the other points of the field of vision. The initial level of stimulus intensity for the points surrounding one of the four points primary, is calculated from the values obtained at the primary point itself and the slope of the vision in that area. From this point on,

procedure 4-2-1 starts, and the following starting levels are calculated as the average values of the three-point thresholds close to the point to be tested (Figure 2.8) [23].

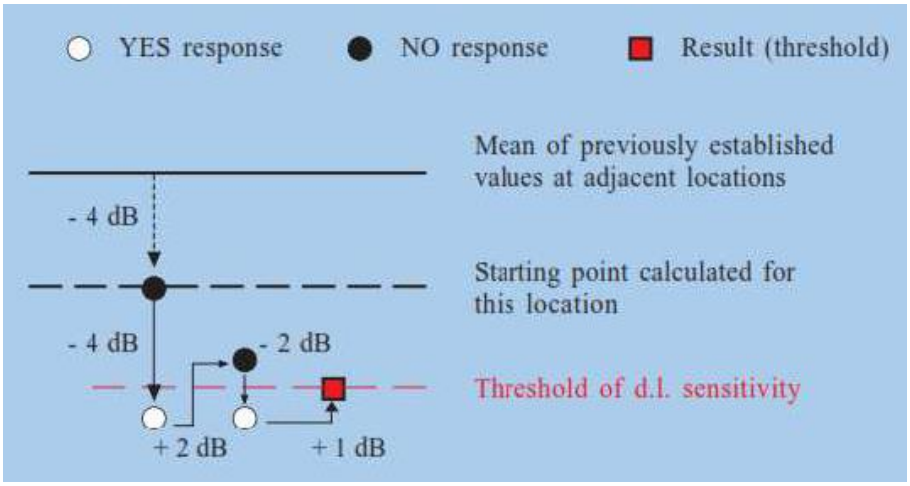

Figure 2.8: Diagram of the 4-2-1 dB strategy for determining the threshold.

2.5.2 SITA Strategy

SITA stands for Swedish Interactive Threshold Algorithm. This algorithm, developed for the Humphry (HFA) perimeter a medical device in ZEISS, uses a complex mathematical model to estimate threshold values at each point of the HFA perimeter field of vision.

It bases the estimate on responses obtained from stimuli presented at that point, but also on information from points adjacent to this one. The thresholds are still determined using the method a full threshold described above, at the four main points (one in the middle of each quadrant). These values are then used to calculate the intensity level of the initial stimulus to be applied to nearby points. The patients' responses to projected stimuli, and a priori distributions that are known, are used for calculating Bayesian probability distributions a-posteriori. The a-priori distributions are nothing more than the normative database, i.e. models of the fields of view of healthy and unhealthy patients available thanks to the enormous amount of data that has been collected over the years. These models take age into account and describe the distribution of thresholds that can be considered a priori information. But it is not enough, the model also includes information on FOS-curves (frequency-of-seeing curves) and correlations between the different points on the grid. The FOS-curves describe the probability that the patient will give a positive answer to the various intensities of stimuli presented in that position. The sensitivity value obtained in correspondence of a 50% probability of this curve, is nothing more than the threshold. It is therefore understood that the slope of such curves is

important: a reduced slope is characteristic of a curve whose course is steep and therefore of a well-defined threshold value, conversely a greater slope is characteristic of a curve flatter and therefore with a less defined threshold value [24].

Correlations between variations in threshold values are greater between adjacent points than between distant points, both in the case of normal and glaucomatous patients. In the latter case the depressed points tend to be placed within clusters that correspond to the anatomy of the fibres of the optic nerve [24].

The a priori model uses two maximum likelihood functions (MAP estimation) for each point on the grid: the two curves, one for normal points and the other for abnormal points, describe the probability of estimated threshold values. These probability functions are periodically updated to depending on the answers given by the patient during the test. The MAP estimation method is used to find the best classification, i.e. to discern whether the patient is glaucomatic or not. The time of a test performed with such an algorithm, in normal individuals, is about half as long as a test with threshold full, while reproducibility is maintained or improved [24].

2.5.3 ZEST Strategy

The Zest strategy is the one on which the attention was focused for the determination of this project. While the full threshold strategy is the oldest and was widely used in the past, the focus has shifted to new strategies that can reduce the total acquisition time of the diagnostic examination. SITA standard and SITA fast are the two strategies on which not much information is available, so CenterVue has tried to implement the ZEST [25].

Zippy Estimated by Sequential Testing (ZEST) is based on a Bayesian decision algorithm: the combination of the knowledge obtained from each stimulus performance and a-priori knowledge about the distribution of thresholds (probability density function (PDF)). The intensity of the stimulus proposed is the result obtained by the mean of PDF, i.e. the combination between previous functions and the initial PDF [25, 26].

This technique is different from staircase strategies because it does not limit the intensity level: the perimeter design will contain the realizable intensities of stimuli.

Zest begins with a function that describes where threshold values are likely to lie in the population called the prior PDF. Modifying the PDF derived from empirical data is possible to implement the ZEST strategy [26].

The mean of this prior PDF returns the most likely estimate for threshold and corresponds to the intensity presented to the subject. After the subject has responded to the presentation, Bayesian logic returns a posterior PDF from the prior PDF by having the likelihood function associated with the response modify the prior PDF as follow [26]:

Posterior PDF = (prior PDF) x (likelihood function)

This posterior pdf becomes our best estimate of the threshold domain for the particular response. It also becomes the new prior pdf for our next presentation and the mean of this modified prior pdf provides an unbiased estimate of the subject's threshold. The next stimulus is presented at this mean value and the process continues until terminated by some criterion (Figure 2.9) [26].

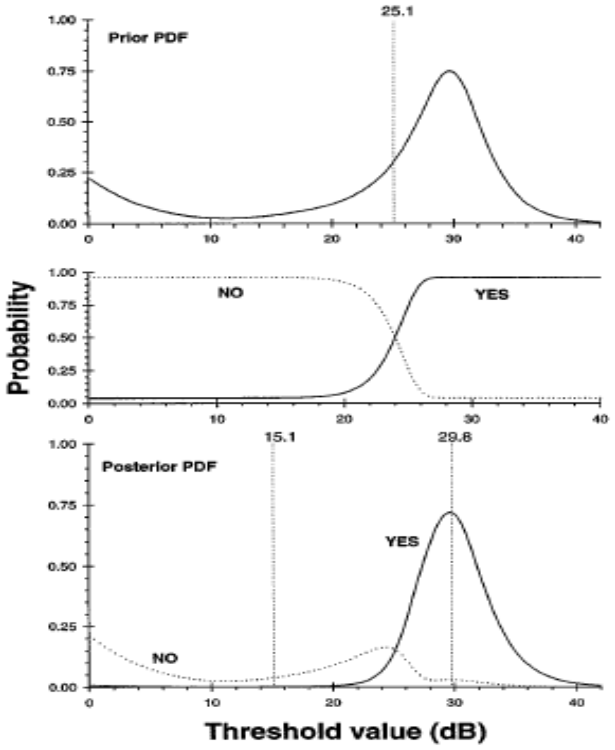

Figure 2.9: A scheme of the first step of ZEST procedure. In the first is shown the prior bimodal pdf derived in a subset of 150 people and its mean (the vertical line). The mean intensity is presented to the subject and results in a response either seen (YES) or not seen (NO) whose likelihood function is shown in the scheme in the middle of the figure (YES solid line, NO dotted line) [26].

The probabilistic functions led to an examination that proved to be very long and tiring for the subject of the acquisition. In addition, depending on the age of the patient in the area where the light stimulus was projected, the examination always fell in the same points tested while using a multiplication between probabilistic curves.

Therefore, CenterVue approximated this Bayesian strategy by proposing binary decision trees. The principle is as follows: there are 6 different levels of intensity that are proposed to the subject on the basis of the patient's age and the ocular area in which he or she finds us during the projection of the stimulus (i.e. macula, right high zone, left high zone, right low zone and left low zone) (Figure 2.10). The initial intensity of the tree represents the root of the tree from which the edges branch off. The diagram that best summarizes this procedure is the one shown in the table.

The age ranges in which the patients have been divided are three:

- From 20 to 50 years
- from 51 to 60 years
- from 61 to 90 years.

This subdivision is based on a data collection in a normative database formed over the years thanks to a collaboration with the San Paolo Hospital in Milan.

The ranges were defined because the population analysed had common characteristics.

Six decision trees were created, each starting at an intensity level of 23, 24, 25, 26, 27, 28 (Figure 2.11, Figure 2.12). The points that are randomly tested in grid 24-2 initially present a level of luminous intensity equal to the root of the initial tree, which depends, as specified above, on the age of the patient and the area of the grid in which the patient is located (Table 2.1).

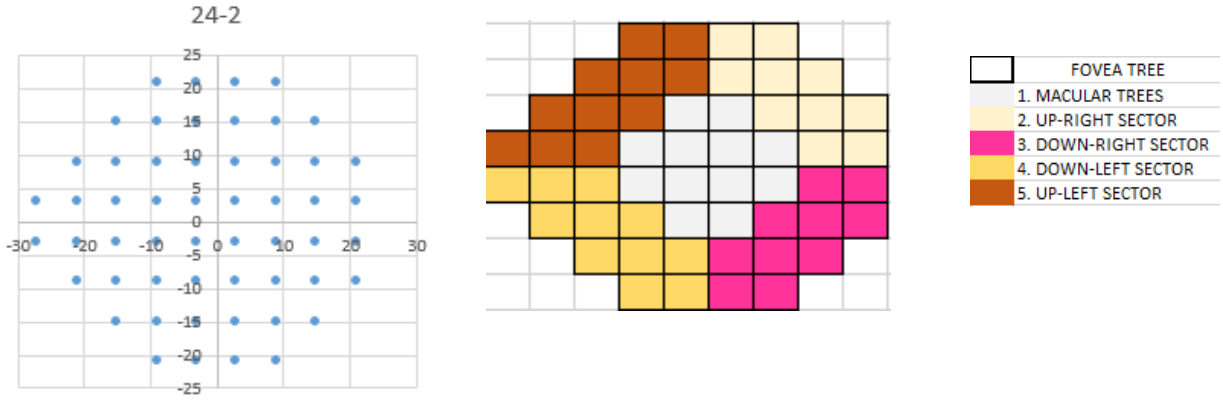

Figure 2.10: Zoning for the implementation of the Zest with control. The grid is based on the standard 24-2 grid.

AGE CLUSTERS		ROOTs of Trees				
1st	20-50	28	24	26	26	25
2nd	51-60	27	23	25	25	24
3rd	61-90	26	23	25	25	24

Table 2.1: Table showing the division according to patient's age and eye area.

If the stimulus is seen by the subject, we move to the right side and a higher intensity is proposed than the previous one; otherwise if the stimulus is not seen we move to the left side tree and the new intensity presented will be lower. The algorithm continues until we reach the "leaf" nodes that estimate the subject's threshold at that point.

There is no predetermined algorithm like full threshold strategies where each tested point is increased or decreased by 4 dB or 2 dB based on the vision of the stimulus. The proposed intensities have been calculated on the basis of probabilistic curves and each tree is unique because it does not have a fixed scheme.

The most interesting points from a diagnostic are when the intensity is -1 dB or 0 dB, respectively corresponding to complete blindness or glaucoma. A control was subsequently introduced for the first nodes of the tree: due to the high subjectivity of the examination, "control" nodes indicated by the blue arrow (Figure 2.11, Figure 2.12) have been inserted to confirm the patient's response. This allowed for a significant reduction in errors.

Therefore, in conclusion, the decision tree works in such a way as to estimate the sensitivity threshold of a patient undergoing diagnostic examination. On the basis of two decisions (YES or NO) corresponding to two branches of the tree (right green for yes and left red for no) it is possible to continue to obtain the threshold.

The tree nodes (Figure 2.11, Figure 2.12) are formed by the key that identifies the intensity level proposed for each step and the index to which they refer.

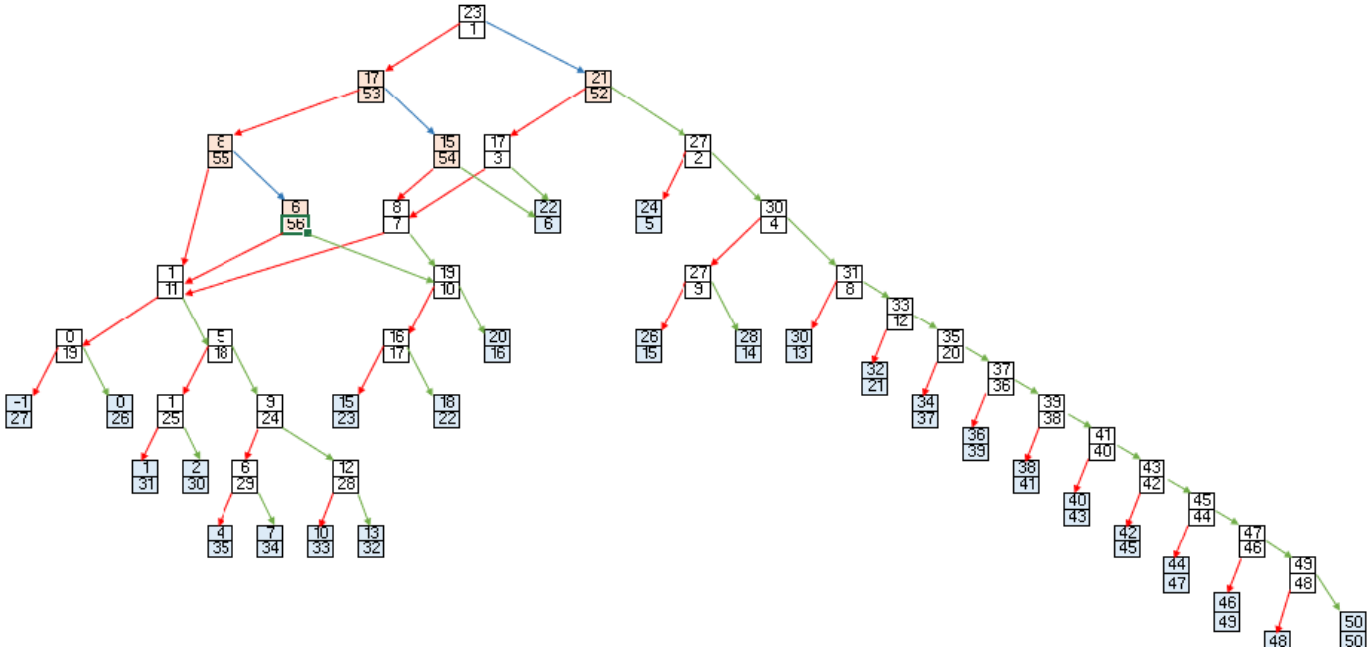

Figure 2.11: Decision tree with root 23 dB for Zest procedure.

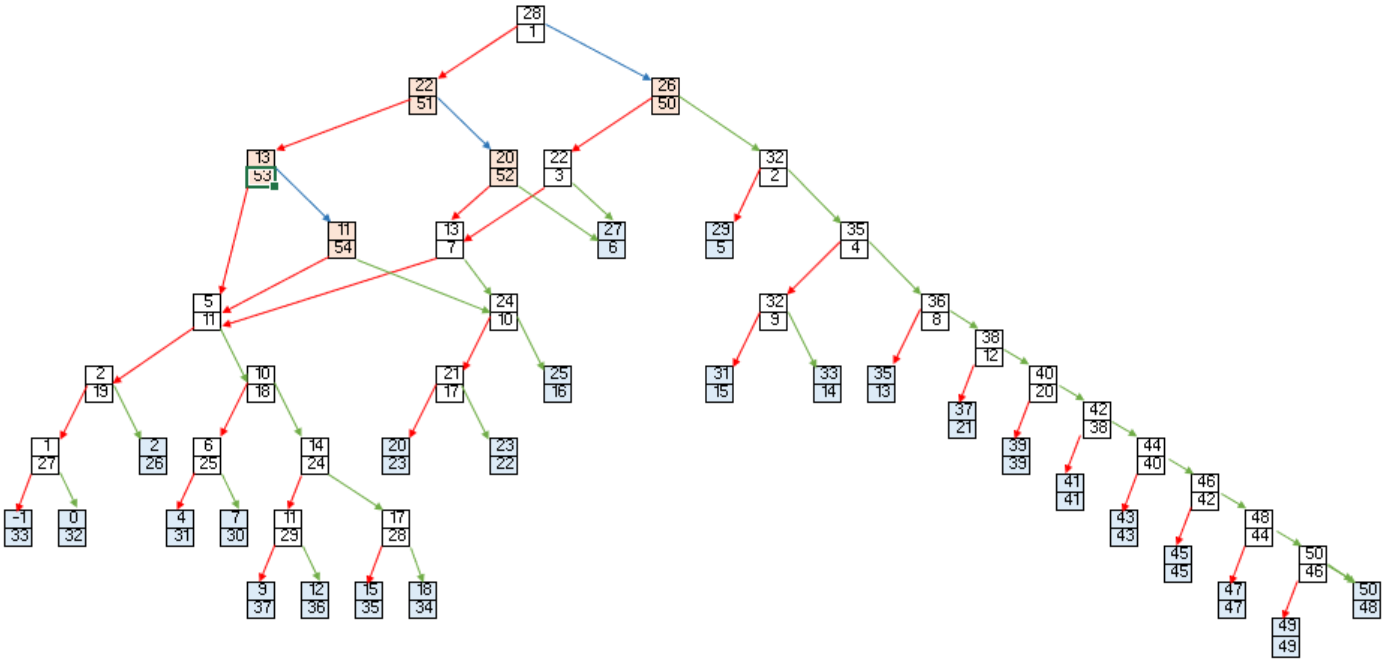

Figure 2.12: Decision tree with root 28 dB for Zest procedure.

3 Simulation with virtual patients

3.1 Compass

The medical device used for this project is Compass. In particular, inside this medical device are defined different strategies for the acquisition of the visual field [27,28].

Compass (Figure 3.1) is a fundus automated perimeter that CenterVue launched in the market between the end of 2014 and the beginning of 2015 [27, 28].

The medical device corresponds to a scanning ophthalmoscope combining to an automatic perimeter, named Fundus Perimeter, that allows the acquisition of confocal images of the retina, simultaneously to the measurement of retinal threshold sensitivity and the analysis of fixation. The Device operates without the need of pharmacological dilation [27,28].

There is full compatibly with standard 24-2 visual field testing and contains an age-matched database of retinal sensitivity in normal subjects. Besides, COMPASS uses a confocal optical design, and it is able to capture color as well as red-free images of superior quality [28]. Moreover, a high-resolution live image of the retina obtained using infrared illumination is available throughout the test. The perimeter is intended for use as a diagnostic device to aid in the detection and management of glaucoma. The device is indicated for measuring retinal sensitivity, for a quantitative assessment of fixation characteristics, as well as to capture infrared and color images of the retina without the use of a mydriatic agent [28].

The clinical interpretation of the COMPASS exam is restricted to licensed clinicians. The process of making a diagnosis using COMPASS results is the responsibility of the eye care practitioner. Another characteristic is the live image obtained using infrared illumination.

Figure 3.1: Compass [29].

3.1.1 Retinal tracking

Thanks to infrared images, acquired at the rate of 25 images per second, is possible to track continuous, automated, the eye movements with positional accuracy in the 10-20 microns range (Figure 3.2). Determination of eye movements yields to Fixation Analysis, where the location of the functional site of fixation and its stability are computed. Fixation analysis is unique to Fundus Automated Perimetry [28].

Retinal tracking also yields to active compensation of fixation losses, with perimetric stimuli being automatically re-positioned prior to projection based on the current eye position. This mechanism is critical to reduce test-retest variability and ensure accurate correlation between function (i.e. retinal threshold values) and structure (retinal appearance). Compensation of eye movements takes place before and during the projection of a certain stimulus. In absence of this mechanism, a normal 2-3 degrees shift in eye position occurring at the time of projection of a certain stimulus would easily produce an artifact in VF results, with a wrong sensitivity being reported at that specific location [28].

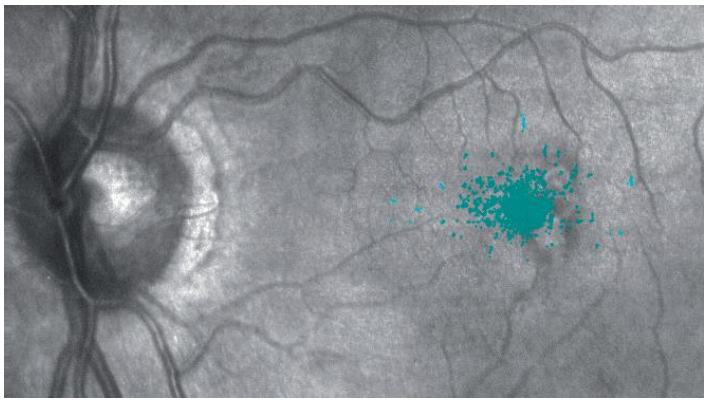

Figure 3.2: Plot of eye movement during the visual field test [28].

3.1.2 Color confocal imaging

Compass uses white light instead of monochromatic lasers, hence providing true color images and offering high fidelity to real retinal appearance. Compass images improve the diagnostic capabilities in the management of glaucoma as they offer:

• no need for pupil dilation

• excellent resolution and contrast

• high quality even in presence of media

opacities, such as cataract

• optimized exposure of the ONH

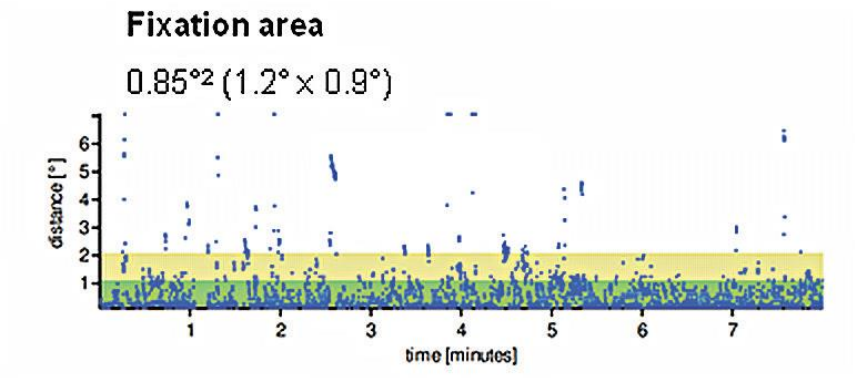

Figure 3.4: Fixation behaviour in glaucoma open angle.

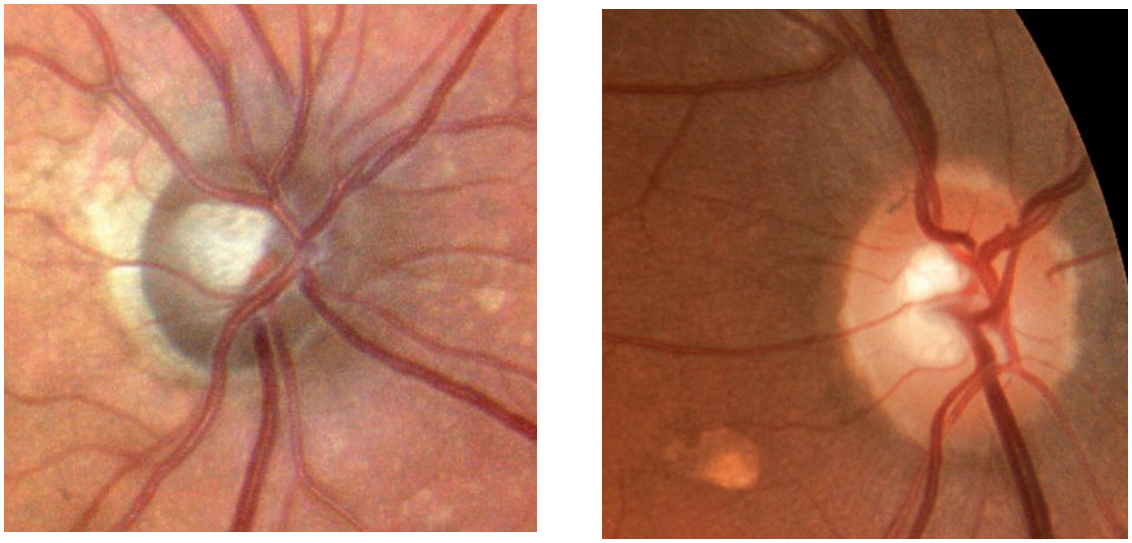

Figure 3.3: (on the left side) Colour detail of ONH, (On the right side) Non-confocal imaging detail of the ONH [28].

3.1.3 Fixation Analysis in Glaucoma

Studies have demonstrated abnormal fixation characteristics in patients diagnosed with early Primary Open Angle Glaucoma (POAG) and Advanced Glaucoma without other retinal diseases. For example, fixation instability has been demonstrated in early and moderate POAG, while other studies have reported predominantly eccentric fixation in up to 15% of the studied population with advanced glaucoma (Figure 3.4). Finally, it is known that fixation stability and its location correlate with visual acuity, in particular the more unstable and eccentric fixation is, the lower visual acuity. Fixation analysis with Compass provides additional, quantitative, parameters for assessing visual function (Figure 3.5) [27,28].

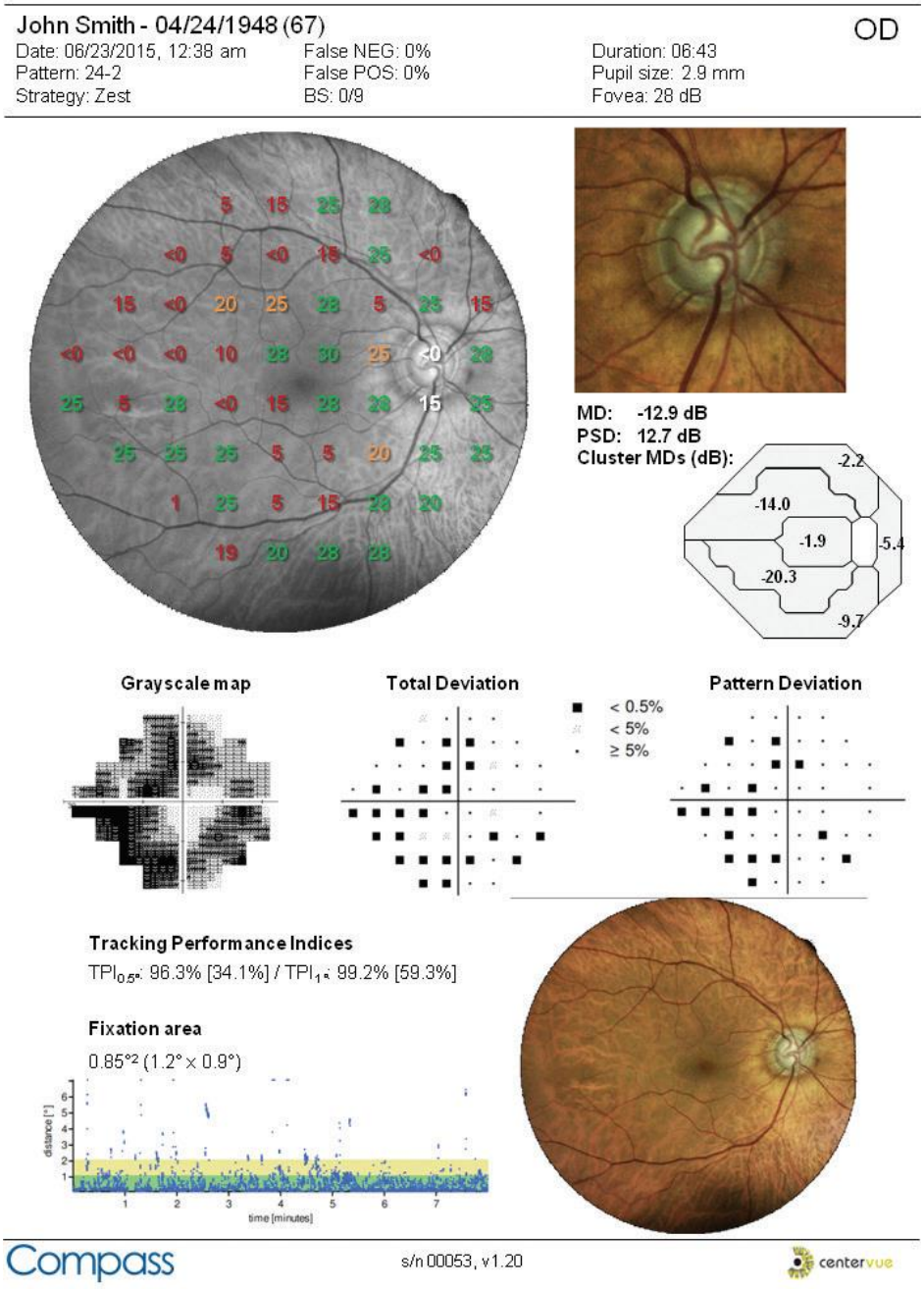

Figure 3.5: Compass Printout [29].

3.2 Threshold sensitivity in terms of stimulus intensity

Each point in a patient's field of vision has its own threshold of visual sensitivity. A stimulus cannot be perceived if it is weaker (less intense) than the threshold stimulus: it is therefore an under-threshold stimulus. All stimuli that are stronger (more intense) than the threshold stimulus is perceivable at each location, they are over-threshold.

The perception of a stimulus depends on characteristics such as intensity, luminance of the background, size of the aim, etc. At the boundary between visibility and non-visibility, the patient's responses are uncertain or consistent: when determining the lower bound and the upper bound of the point where there is the actual sensitivity of the patient. When the intensity of the proposed stimulus is within this region, it can be increased so that the patient will respond to having seen it 25% of the time, at a slightly higher intensity the patient will respond 50% of the time. If the responses are carefully determined, the threshold of sensitivity is defined as the intensity of the stimulus to which the patient will respond 50% of the time (Figure 3.6).

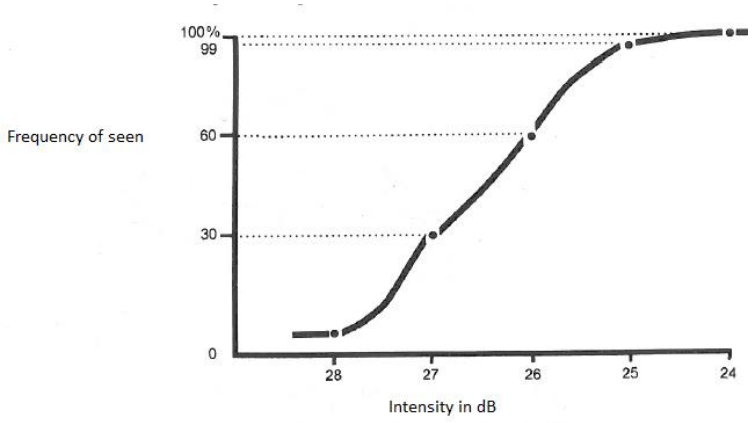

Figure 3.6: Frequency of seen curve.

Therefore, if a stimulus has an intensity close to the patient's threshold, it is perceived as a rather weak stimulus barely visible. When it is more intense, it appears brighter and it is easier to perceive it with certainty. The more intense it is, the easier it is to see it. Many patients, however, say that many stimuli presented during the threshold test are rather weak. Watching weak stimuli makes the diagnostic test difficult and tiring. Visible or invisible stimuli produce the patient's fear of making mistakes. In addition, there is a high level of subjectivity derived from the length of the examination that causes the patient fatigue and loss of concentration. There

are also cases of happy trigger: patients who press the push-button even if they do not see the stimulus [23].

3.3 Idea of the project

In order to decrease the high subjectivity given by the examination with the patient for the reasons discussed above, the idea behind the thesis project is to simulate a model of virtual patients to test and compare the performance of strategies for the acquisition of the visual field.

Knowing a priori the characteristics of the patients, after testing the sensitivity through the strategies it is possible to verify which strategy is the best in terms of acquisition time and error.

All the components used and created through MATLAB will be discussed in detail below.

3.3.1 Object Oriented Programming (OOP)

Object-oriented programming is a programming approach that associates data and methods on a logical structure called object. MATLAB is a very frequent programming structure being able to produce complex computer applications. OOP uses:

- Class definition files, enabling definition of properties, methods, and events.
- Classes with reference behaviour, helping the creation of data structures such as linked lists.
- Events and listeners, allowing the monitoring of object property changes and actions.

A class is an "*Abstract Data Type*" (ADT, Abstract Data Type) that is an entity characterized by a domain of values (that is, a set of possible values that the entity can assume) and by an algebra on such domain (that is, a set of possible operations on such set) [30].

In a class, the domain is composed of all the attributions (i.e., all the properties that characterize the class) while operations on attributes can be performed by the user by invoking appropriate methods of the class (i.e., the user calls up specific functions of that class).

At this point, I can define an object of a certain class C as an instance (i.e., a member, a representative) of that Class C. Obviously, object will inherit all attributes and methods of class C. The value assumed by the attributes of obj will define their status, the obj methods will correspond to the possible operations on the object (e.g., I can invoke the obj to read or modify its attributes) [30].

3.3.2 Patients definition

Using object-oriented programming in MATLAB, it was possible to create several related classes with functions defined within a main code.

The patients that have been simulated are of 5 different types: *Normal* patients, *Random* patients, *Flat* patient, *Blind* and *Perfect average* patients.

The characteristics to create these patients have been obtained from the normative database of data collected over time thanks to the collaboration with the hospital of San Paolo in Milan. Through the processing of the collected data it was possible to define the level of average sensitivity according to the type of patient and the age he/she presented. In fact, as mentioned before, this subdivision is made on 3 main ranges: from 20 to 50 years old, from 51 to 60 y/o and from 61 to 90 y/o.

However, it was not possible to simulate glaucomatous patients because the glaucoma pathology is very difficult to predict as it does not degenerate according to a precise pattern. Although we have data from glaucoma patients, its simulation is impossible to do because it is random. This is the reason why only healthy patients have been considered for the definition of the model.

In detail: these 5 types of patients within the "*Patient Type*" class have been defined. Subsequently, in the Patient Type class, the characteristics taken into consideration for each of the 5 types were defined.

Perfect Average patients have sensitivities exactly equal to those of the normative model of collected data. The sensitivity to the stimulus of the *Normal Patient* is the result of the calculation of mean and standard deviation of the normative model. The sensitivity of *Random* patient was created by generating a vector of random values taken from the normative database through the MATLAB "*randn*" function, while *Flat* patients are the result of a multiplication with a vector of all 1 ("*ones*").

3.3.3 Strategist

In "Strategist" class it was possible to implement a set of strategies that are tested and compared in terms of performance (time and error).

The strategies that have been implemented through MATLAB code are some of those discussed in Chapter 2, in particular: full threshold strategy 4-2, 4-2-1, classic Zest and Zest with cc (control).

Functions have been created within strategists able to randomly select points in grid 24-2 on which to project light stimuli to estimate the patient's threshold.

The structure that has been used for the implementation of all the strategies is "*State Flow Machine*". Each strategy can be seen as a decision tree: Zest seen in chapter 2 has been approximated as a tree to exemplify its procedure, full threshold strategies can be implemented as a recursive binary decision tree: depending on whether a stimulus is seen or not, each node of the tree is respectively increased or decreased by 4 dB or 2 dB or 1 dB until the sensitivity threshold is detected.

3.3.4 4-2 Full Threshold

Each grid index is tested randomly. Then the state flow structure is used, through a series of "*switch...case*" switches all grid points are tested reaching a threshold level.

In detail, we have initialized a variable called "*staircaseStatus*" which is updated at each iteration and which is used to detect the increase or decrease of intensity in dB (Figure 3.8).

There are two possibilities when a stimulus is proposed: seen stimulus or not seen stimulus. If a stimulus is seen, then the intensity increase by 4 dB until the stimulus becomes so bright that it is no longer visible to the patient. When a stimulus is not seen, it is decreased by 4 dB. If the stimulus has been seen and therefore a value equal to 4 dB has been added to the initial intensity proposed, then there are two other possibilities depending on whether it is seen or not, which correspond respectively to an increase of +4 dB or a decrease of - 2 dB. The algorithm continues discussing and testing each case until the last stimulus presentation that represents the patient's estimated threshold (Figure 3.8).

In the code (Figure 3.7) the "cases" discussed are the integers corresponding to the dB increase or decrease: +4, -4, +2, -2. From a formal point of view, each tree represents a node from which

two other nodes branch out. When you reach the leaf node, which corresponds to *staircaseStatus = 0*, you have reached the sensitivity threshold.

```
switch staircaseStatus(ind)


case +4
        if ~seen
        intensities2beProposed( ind ) = intensities2beProposed( ind ) - 2;
        staircaseStatus(ind) = -2;
        else
        intensities2beProposed( ind ) = intensities2beProposed( ind ) + 4;
        end

case -4
       if ~seen
       intensities2beProposed( ind ) = intensities2beProposed( ind ) - 4;
       else
       intensities2beProposed( ind ) = intensities2beProposed( ind ) + 2;
       staircaseStatus(ind) = +2;
       end

case -2
        if ~seen
        intensities2beProposed( ind ) = intensities2beProposed( ind ) - 2;
        else
        intensities2beProposed(ind)= intensities2beProposed (ind);
        estimatedThresholds(ind) = intensities2beProposed( ind );
        staircaseStatus(ind) = 0;
        end

case +2
       if ~seen
       intensities2beProposed( ind ) = intensities2beProposed( ind ) - 2;
       estimatedThresholds(ind) = intensities2beProposed( ind );
       staircaseStatus(ind) = 0;
       else
       intensities2beProposed(ind ) = intensities2beProposed( ind );
       end


end
```

Figure 3.7: Parts of code representing State Flow Machine for 4-2 Strategy.

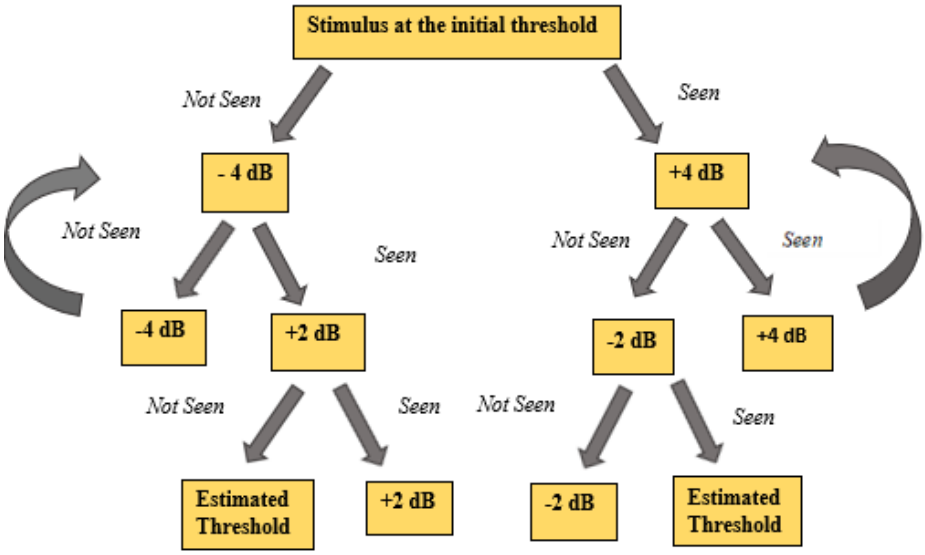

Figure 3.8: Example of a full threshold 4-2 strategy scheme. It exemplifies what is written in the MATLAB code in figure 3.7.

3.3.5 4-2-1 Full Threshold

The principle is the same as strategy 4-2 but with an adjustment of +/- 1 dB (Figure 3.10) if the stimulus is seen or not. In the code, this varies simply by adding two more cases, respectively +1 and -1 (Figure 3.9).

```
…

 case -2
   if ~seen
   intensities2beProposed( ind ) = intensities2beProposed( ind ) - 2;
   else
   intensities2beProposed(ind)= intensities2beProposed (ind) + 1;
   staircaseStatus(ind) = + 1;
   end

 case +2
   if ~seen
   intensities2beProposed( ind )= intensities2beProposed( ind ) - 1;
   staircaseStatus(ind) = -1;
   else
   intensities2beProposed( ind ) = intensities2beProposed( ind ) + 2;
   end
 case +1
   if ~seen
   intensities2beProposed( ind ) = intensities2beProposed( ind ) - 1;
   estimatedThresholds(ind) = intensities2beProposed(ind);
```

```
    staircaseStatus(ind)=0;
    else
    intensities2beProposed( ind ) = intensities2beProposed( ind ) + 1;

case -1
   if ~seen
   intensities2beProposed( ind ) = intensities2beProposed( ind ) - 1;
   else
   estimatedThresholds(ind) = intensities2beProposed( ind );
   staircaseStatus(ind) = 0;
   end

end
```

Figure 3.9: Partial code for 4-2-1 strategy. As we noticed, there are two additional cases discussed correspond to +1 dB and -1 dB.

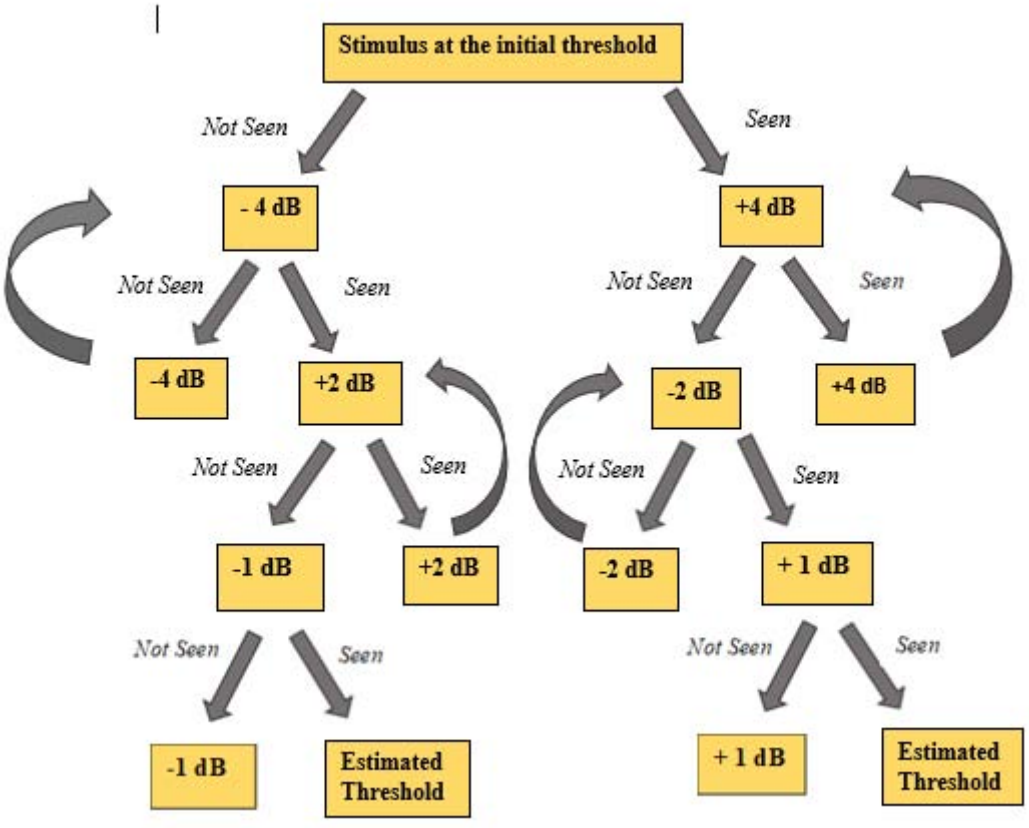

Figure 3.10: : Example of a full threshold 4-2-1 strategy scheme. It exemplifies what is written in the MATLAB code in figure 3.9.

3.3.6 Zest

Strategy defined within the class *"Strategist*". First, as already described in Chapter 2, we defined the criterion according to the intensity proposed to the initial stimulus. Then a function named "*Guess Zone*" was created, external to the Strategist class, which gave the grid indices as input, returning the reference zone corresponding to the input index (Figure 3.11).

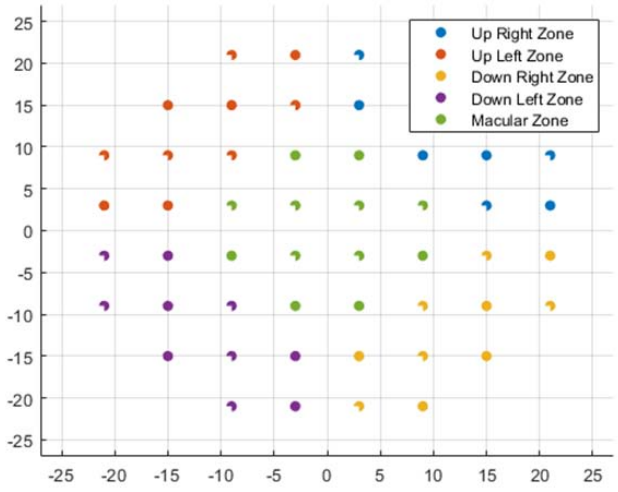

Figure 3.11: Division of indices per zone. Each point in the grid has coordinate point (x,y) of an index, and each index belongs to a region that is considered for the projection of a certain level of intensity.

Next, an additional function was defined named "*PP_Zest*": depending on the zone in which we are located (determined by the previous function "*Guess Zone*") and the age of patients, the output of the function returns the tree root (defined as a string) from which we have to start. The trees of Zest strategy are 6 and they are identifiable thanks to the different root of each tree: 23, 24, 25, 26, 27, 28. All this has been applied in the Strategist class, in particular in the part of the code dedicated to which one intensity is proposing in the various points of the grid.

Once determined how and what kind of intensity to project at various points on the 24-2 grid, the Zest strategy was implemented.

Using the principle of the State Flow Machine, considering that a numerical approach such as 4-2 or 4-2-1 was not good because the proposed dBs were not unique but were repeated in various tree nodes, it was decided to use strings.

Each string is unique and identifies only one node of the tree: in this way it was possible to create as many cases as there are nodes of the reference tree. Each of the cases with the two possibilities corresponding to "*seen"* and "*not seen*".

Each of the 6 trees has been divided into two sub-trees: right and left. For each sub-tree, visits to the nodes have begun.

Respectively, the nodes have been initialized as right or left according to the sub-tree to which they belong and with a number, referring to the level in which they were located.

For example: the tree root with an intensity of 23 was named as "*root23*", then the two child nodes of the root, corresponding to seen stimulus (right) and not seen stimulus (left) as *node2_dx23*, *node2_sx23*: node belonging to the second level of tree 23, left or right.

Because it is a binary tree, each level has 2^n nodes (with n number of levels), so the third level has 8 nodes called "*node3sx_sx23*", "*node3dx_sx23*", "*node3sx_dx23*", "*node3dx_dx23*" respectively: node on the third left level of the left subtree that has root 23, node on the third right level of the left subtree with root 23, node on the third left level of the right subtree that has root 23 and so on (Figure 3.12).

The nodes, initialized as strings of letters, are contained in a cell structure of length equal to the number of points in the grid (1x54). Each cell is initialized with intensity equal to the intensity of the tree in its root and gradually updates depending on whether a stimulus is seen or not by changing its state.

The final state of the cell will contain the string of the node to which the threshold intensity is associated at that point of the grid.

Through the "*switch...case*" it was possible to create the tree by visiting each node and adding or removing dB on the basis of the trees defined in Chapter 2.

Each "*case*" is represented by a node (defined as a string of letters), the patient's threshold is reached when a tree leaf node is visited.

The "*staircaseStatus*" is a variable initialized after adding or subtracting the proposed intensity and it is important because it is what allows the code to understand if a node has already been tested or not. When "*staircaseStatus*" is different from zero then it means that the tree visit must continue, when it is zero it means that the node in question is a leaf node and corresponds to a threshold.

```
...

case 'root23'

    if ~seen
    intensities2beProposed (ind) =  intensities2beProposed (ind) - 6;
    status{ind} = 'node2_sx23'; %17
    staircaseStatus(ind) =  - 6;

    else
    intensities2beProposed (ind) = intensities2beProposed (ind)  + 4;
    status{ind} = 'node2_dx23';
    staircaseStatus(ind) =  +4;

    end

. . .
```

Figure 3.12: Part of the code exemplifies what specified above: staircaseStatus in this case is different from 0 so the knots considered do not correspond to leaves but to knots that in turn will have two children.

3.3.7 Zest with cc

The strategy called Zest cc, uses exactly the same principle as the Zest strategy described above, with the only difference being the extra nodes added as a control to reduce errors. These nodes have been defined with exactly the same principle of the nodes described in the previous paragraph with the only difference that the two letters "*cc*" have been added to identify them better in the code.

3.3.8 Visual Field Shared Standard

This class holds standards about VF (Visual Field) info and normative data. In particular, always referring to the Zest strategy calculated with curves (Chapter 2), with this class all the characteristics necessary to calculate the normative DB have been defined.

They have been calculated, always referring to grid 24-2 (of 54 points) intercept and angle coefficient.

Then, the standards deviation for each age range were defined for each point of the grid acquired through the normative patient model. After that, 3 different vector measurement matrices (1x54) containing the standards deviations for each point were defined for age between 20 y/o and 50 y/o, age between 51 y/o and 60 y/o and age between 61 y/o and 90 y/o.

Three different curves were then calculated with the data collected.

Referring to the classical equation $y = mx + q$ (where m angle coefficient and q intercept of the curve), the values then used for the calculation of the average of the normative model were the following:

```
mean = slopes * age + intercepts;
```

Therefore, the average of the normative model depends on the age of the patient under consideration: this is given by the slope of the line (angle coefficient whose values were previously defined in the code thanks to the data collected from a healthy population) which is multiplied by the age. The mean is then calculated considering the previous calculation and with the addition of the intercept (that is defined in the first part of the code belonging to this class). In this way it has been possible to have average and standard deviation creating virtual patients with these characteristics.

4 Results obtained and discussion

4.1 General consideration and definition of the project

After defining the classes used, and how the various strategies were implemented, it was possible to apply them to virtual patients.

The purpose of the project is to simulate 100 different patients for each age considered: as already mentioned, the ages of the patients considered are from 20 to 90 years divided into 3 different ranges (from 20 to 50 years from 51 to 60 and from 61 to 90). The general age range extends in a vector ranging from 20 to 90 years for a length equal to 71 units.

Projecting 100 patients for each age, the result is a model of 7100 simulated patients. The previously defined strategies (see Chapter 3) were applied to all these patients and could be compared in terms of number of projections and mean squared error (MSE). The indices considered for the comparison of the strategies are those most used in perimetry.

The fundamental characteristics for a good visual field acquisition strategy are the accuracy of the examination and the total time of the diagnostic examination.

In perimetry, considering that the majority of patients are elderly, a long examination (in terms of time) but accurate is tiring for the subject who often loses concentration often invalidating the check-up; on the other hand, a strategy that estimates points of sensitivity of the visual field with a high level of error but that lasts a short time is lighter for the patient but produces a diagnostic examination absolutely not accurate and precise. A compromise is therefore required between the duration of the examination in terms of time and acquisition accuracy.

The goal of the thesis is to compare different strategies used in COMPASS to see which one is the best.

The added value of this method is the simulation of virtual patients: the problem of subjectivity of the diagnostic examination is solved by using simulated patients, created in such a way that their response is always true and verified.

During an examination with COMPASS, often there are two scenarios: a luminous stimulus that is projected is seen by the patient who does not press the push button, or, in the other hand, the luminous stimulus is not seen but the patient presses the push button. When you present a bright stimulus to a patient and wait for his response, you are never absolutely sure of the

truthfulness of the result obtained. The new method of simulation of virtual patients is able to overcome this problem because the intrinsic characteristics of the patients considered are known. Therefore, not having the obstacle of the "uncertain" answer, the attention is focused more deeply on the performance of the strategies trying to obtain the best result.

The purpose of the simulation is to develop new strategies for the projection of light stimuli allowing to evaluate their performance compared to the algorithms currently implemented and used in clinical practice. In particular, in the future, new strategies will be researched that will reduce the examination time and keep the measurement reliable. In addition, these strategies will be validated by generating thousands of virtual patients who have certain reference characteristics (i.e. whose simulated field of vision is similar to a healthy profile or affected by specific types of retinopathy). This is important, because the validation of algorithms in the clinic is long and expensive: normally it is necessary to recruit subjects prepared to do the visual field several times, and there is no prior knowledge of how reliable people are in doing this examination. Consequently, it is important to be able to simulate any software modification that impacts the performance of the instrument, before validating it in the clinical field.

For a question of similarity, considering that the strategies developed are four (Full Threshold 4-2, Full Threshold 4-2-1, Zest and Zest with cc) we wanted to compare two strategies per time. We then have the comparison between Full Threshold 4-2 and 4-2-1, Zest and Zest with cc and finally since both are used in COMPASS currently, Zest with Full Threshold 4-2.

4.2 Mean Squared Error and total number of projections

As explained above, a vector length of 7100 patients was obtained, i.e. 100 patients for each age from 20 to 90 years. Subsequently, an "*Exam_Visual_Field*" function was created in MATLAB that gives the type of strategy to be considered and the type of patient, returns the number of projections and the mean squared error.

The number of projections is "how many times a grid point is tested", clearly the more they are the longer the field of view acquisition time.

The mean square error is defined as follows: $$MSE = \frac{\sum_{i=1}^{n} (x_i - \widehat{x}_i)^2}{n}$$

In statistics, the quadratic mean error (MSE) indicates the mean square discrepancy between the values of the observed data and the values of the estimated data. In particular, the true value given by the sensitivities obtained from the normative patient DB and the sensitivities obtained from the virtual patient model were considered.

Then the mean quadratic error was initially calculated on 100 simulated patients obtaining an MSE value for each age from 20 to 90 years (i.e. 71 values per MSE). Subsequently, since 3 different age ranges have been defined, the MSEs for each age range have been calculated obtaining 3 final results reported in the tables below.

4.3 Comparison between 4-2 and 4-2-1 strategies

In this paragraph, are compared the two strategies that present exactly the same algorithm but differ by an adjustment of 1 dB that is added or subtracted from the last seen stimulus (defined as the patient's threshold).

The Full Threshold 4-2 strategy is used within COMPASS (Chapter 3) and is one of the most commonly used strategies in the past in perimetry. The Full-Threshold 4-2-1 strategy with the addition of +/1 dB was dropped because it used too many projections.

Both strategies were applied to the model of virtual patients as explained above. The graphs obtained through MATLAB are shown below (Figure 4.1 and Figure 4.2).

The difference between the two strategies is evident in Figure 4.1, where the x-axis shows the number of patients and the y-axis shows the average MSE (Mean Squared Error) for each age, the Full-Threshold 4-2-1 strategy is more precise (because it has a lower error) than the Full-Threshold 4-2 strategy. This result, as expected, is because of the +/- 1 dB adjustment which helps to calculate a more precise threshold.

Figure 4.1: Plot of results obtained. Comparison of Full Threshold 4-2 strategy (Blue line) and Full Threshold 4-2-1 Strategy (Magenta line) in terms of MSE (Mean Squared Error).

Showing the results obtained, the mean of MSE was calculated for each age range for both strategies. As can be seen from tables 4.1 and 4.2, the Full-Threshold 4-2-1 strategy is much more precise than the 4-2: it has an MSE in the range of 0.51-0.52 while the 4-2 has a very high MSE.

4-2 Strategy	**MSE [dB]**	**STD**
20 - 50 y/o	1.005	±0.159
51 - 60 y/o	1.002	±0.131
61 - 90 y/o	1.007	±0.171

Table 4.1: Results for Full Threshold 4-2 strategy for each range.

4-2-1 Strategy	**MSE [dB]**	**STD**
20 - 50 y/o	0.252	± 0.052
51 - 60 y/o	0.251	±0.058
61 - 90 y/o	0.252	±0.042

Table 4.2: Results for Full Threshold 4-2-1 strategy for each range.

The trend for both strategies is very similar because it is the same algorithm that is implemented.

As for the number of projections, Figure 4.2, the Full-Threshold 4-2 definitely has less of them, so it is faster. While the Full-Threshold 4-2-1 has a higher number of projections and takes longer. The results are reported in table 4.3 and 4.4.

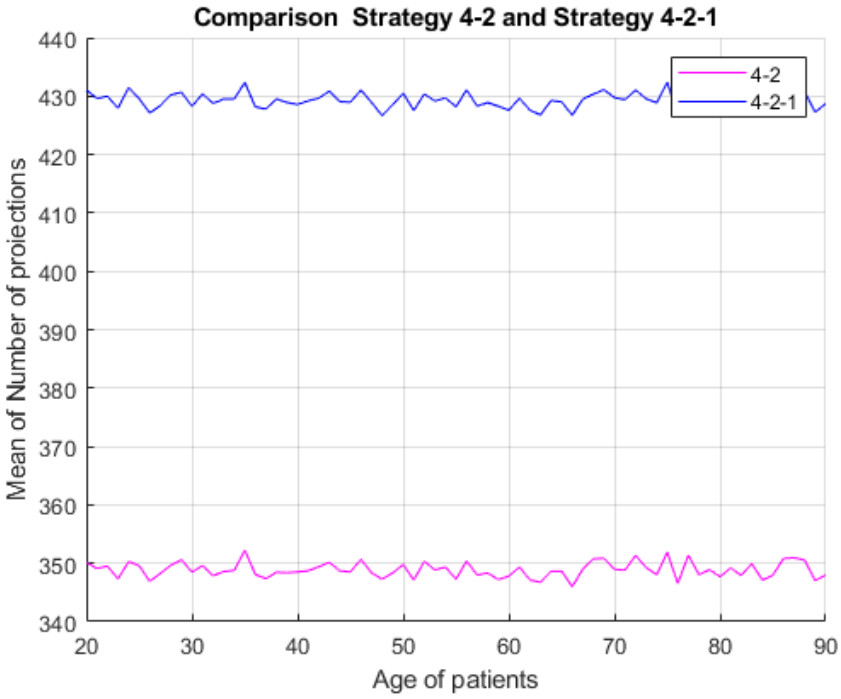

Figure 4.2: Plot of results obtained. Comparison of Full Threshold 4-2 strategy (magenta line) and Full Threshold 4-2-1 Strategy (blu line) in terms of number of projections.

Full Threshold 4-2	**Mean number of projections**
20 - 50 y/o	366.8
51 - 60 y/o	354.2
61 - 90 y/o	368

Table 4.3: Results obtained in terms of number of projections for each range of age.

Full Threshold 4-2-1	**Mean number of projections**
20 - 50 y/o	448.1
51 - 60 y/o	436.1
61 - 90 y/o	446.9

Table 4.4: Results obtained in terms of number of projections for each range of age.

4.4 Comparison between Full Threshold 4-2 and Zest

The two strategies considered in this paragraph are those used within COMPASS (Chapter 3).

The Full-Threshold 4-2 strategy is one of the first strategies used for VF (Visual Field) acquisition before the introduction of bayesian strategies (such as the Zest). It is possible seeing positive and negative points for both. To underline the differences, graphs have been plotted to summarize their performance. The two graphs obtained are discussed below (Figure 4.3 and Figure 4.4).

Figure 4.3: Plot of results obtained. Comparison of Full Threshold 4-2 strategy (magenta line) and Zest Strategy (blue line) in terms of MSE (Mean Squared Error).

In the first graph (Figure 4.3) the ages of the patients are reported in the abscissae axis while in the ordinate axis the MSE calculated on 100 patients for each age is averaged.

As can be seen, the difference between the Zest Strategy and the Full Threshold Strategy is evident, indeed the Full Threshold strategy has a lower level of precision than the Zest Strategy.

It is concluded that, as clearly visible from Figure 4.3 in terms of error, Zest strategy is better and more precise than 4-2 strategy: the range of MSE is between 0.35 and 0.75 for Zest strategy while for the Full-Threshold 4-2 is higher with a range between 0.96 and 1.04.

The average values calculated for each age range for both strategies are shown in Table 4.5 and Table 4.6.

Zest Strategy	**MSE[dB]**	**STD**
20 - 50 y/o	1.008	±0.1717
51 - 60 y/o	0.965	±0.1678
61 - 90 y/o	0.987	±0.1875

Table 4.5: Results for Zest strategy for each range.

Full Threshold 4-2	**MSE [dB]**	**STD**
20 - 50 y/o	0.5433	±0.5401
51 - 60 y/o	0.5748	±0.4477
61 - 90 y/o	0.5393	±0.7758

Table 4.6: Results for Full Threshold 4-2 strategy for each range.

In order to obtain a more schematic representation between the different performances provided by the two different strategies considered, they are summarized in the two tables (Table 4.5 and Table 4.6). The average errors for each age range, standard deviation and variance have been calculated.

Full-Threshold 4-2 strategy has a greater error but presents a homogeneous trend with positive and negative peaks that differ very little from the average of the total error. Its standard deviation for each age range varies from 0.1717 to a maximum of 0.1875. Considering Zest, it is more precise because it has a lower error but as you can see from the plot of the graph (Figure 4.3) it seems very discontinuous and irregular: it reaches a maximum peak at 0.767 and a minimum peak at 0.322 in the y-axis, so the standard deviation varies from 0.54 to 0.77.

For a more complete analysis of performance, the two strategies were compared by number of projections.

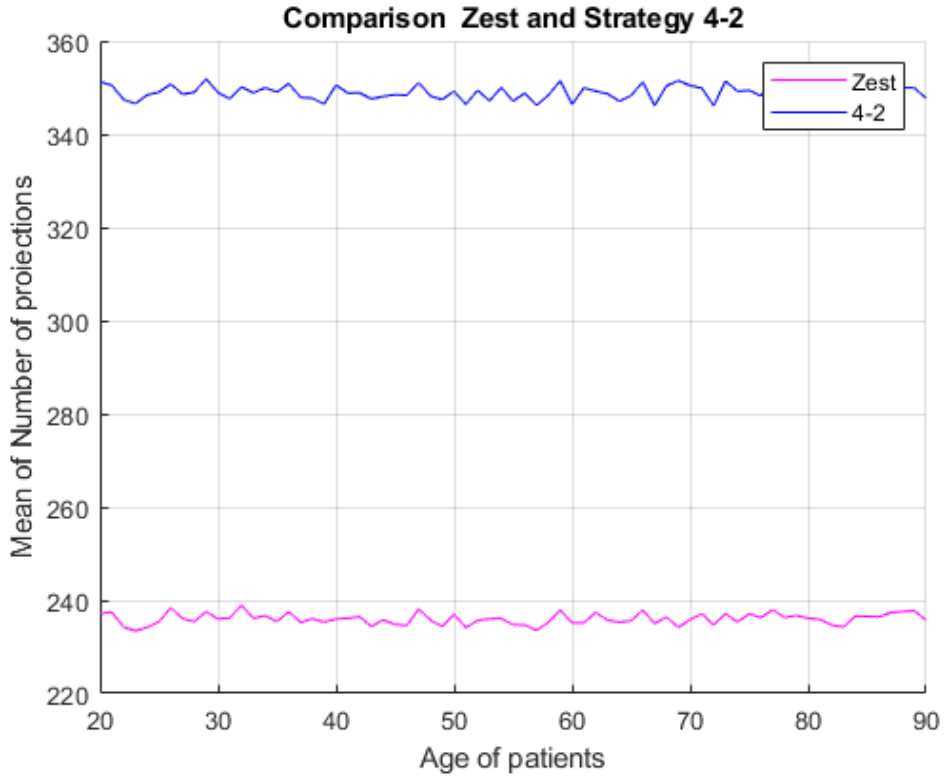

Figure 4.4: Plot of results obtained. Comparison of Full Threshold 4-2 strategy (Blue line) and Zest Strategy (Magenta line) in terms of mean number of projections.

It is evident from the graph in Figure 4.4 that the 4-2 Full-Threshold strategy has a much higher number of projections than the Zest strategy. Indeed, while the first has a number of projections between 340 and 360, the Zest has a much lower number between 220 and 240.

What was expected was obtained: the full threshold 4-2 strategy, as also defined by its name, is very precisely because it tests every point of the grid trying to minimize the range on which the patient sees or does not see the stimulus, through a slight increase/decrease of the proposed dB. Therefore, since the points of the grid are tested several times it presents a higher number of projections than the Zest, causing a not indifferent duration of the diagnostic examination.

To summarise the number of average projections for each age range in a schematic way, the tables below have been defined (Table 4.5 and Table 4.6).

Zest Strategy	**Mean number of projections**
20 - 50 y/o	232.7
51 - 60 y/o	239.6
61 - 90 y/o	235.4

Table 4.7: Results obtained in terms of number of projections for each range of age.

Full Threshold 4-2	**Mean number of projections**
20 - 50 y/o	362.5
51 - 60 y/o	365.8
61 - 90 y/o	362.3

Table 4.8: Results obtained in terms of number of projections for each range of age.

4.5 Comparison between Zest and Zest with cc

As mentioned in chapter 3, Zest and Zest with cc (control) are almost the same algorithm based on binary decision trees with the only difference that Zest with cc has introduced additional nodes in order to test and verify the response of the tested subject.

We wanted to compare these two strategies to evaluate which is actually more effective. As for the previous strategies, the performance was evaluated in terms of MSE and number of projections. The average error was calculated on 100 simulated patients for each age between 20 and 90 years and the results were compared.

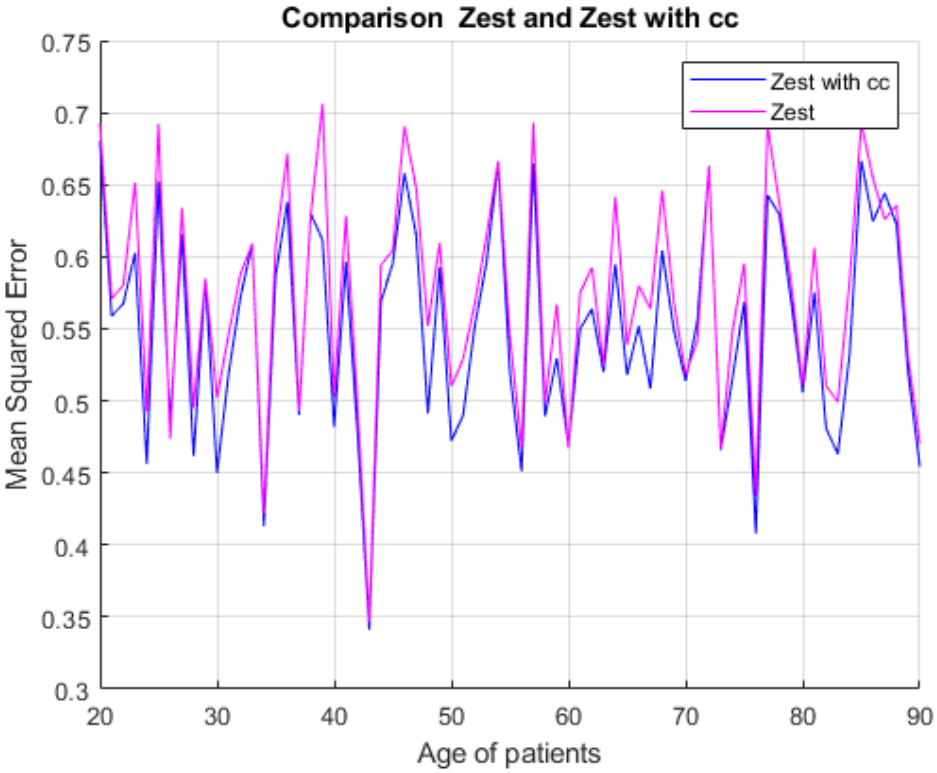

Figure 4.5: Plot of results obtained. Comparison of Zest with cc strategy (Blue line) and Zest Strategy (Magenta line) in terms of MSE (Mean Squared Error).

From the graph shows (Figure 4.5) what stated above. The two strategies are very similar to each other and you can see it from the trend in the graph where in some points the peaks even overlap. However, in terms of error the difference is minimal: Zest with cc has error levels between 0.68 and 0.33 while the Zest has a range between 0.34 and 0.71.

Even if the difference in MSE is minimal, the strategy that has a minor error and is more precise is the Zest with cc (Table 4.9 and Table 4.10).

Zest Strategy	**MSE [dB]**	**STD**
20 - 50 y/o	0.5748	±0.9178
51 - 60 y/o	0.5425	±0.1697
61 - 90 y/o	0.5527	±0.6562

Table 4.9: Results for Zest strategy for each range.

Zest Strategy with cc	**MSE[dB]**	**STD**
20 - 50 y/o	0.5508	±0.8429
51 - 60 y/o	0.5322	±0.1784
61 - 90 y/o	0.5427	±0.7162

Table 4.10: Results for Zest with cc strategy for each range.

The comparison of the two strategies by number of average projections is expressed by the plot shown in Figure 4.6.

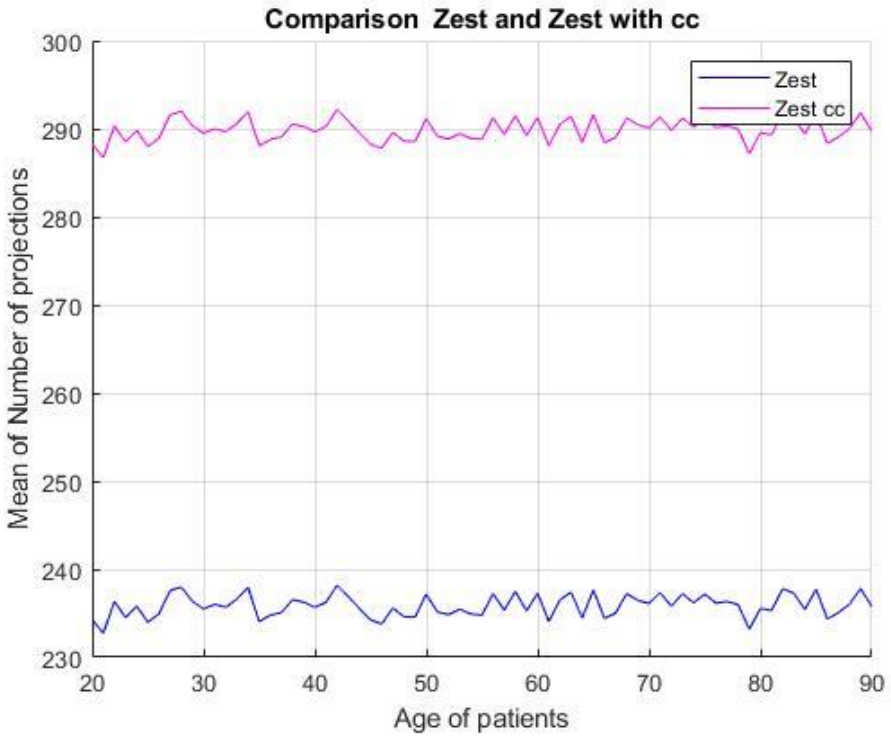

Figure 4.6: Plot of results obtained. Comparison of Zest strategy (Blue line) and Zest with cc Strategy (Magenta line) in terms of mean number of projections.

It can be seen, as expected, that the number of projections is higher for Zest with cc. In fact, since the two algorithms are almost equal, adding nodes to test the grid points several times increases the number of projections (Table 4.11 and Table 4.12).

Zest Strategy	**Mean number of projections**
20 - 50 y/o	239
51 - 60 y/o	235.5
61 - 90 y/o	237

Table 4.11: Results for Zest strategy for each range.

Zest with cc Strategy	**Mean number of projections**
20 - 50 y/o	294
51 - 60 y/o	288
61 - 90 y/o	291.3

Table 4.12: Results for Zest with cc strategy for each range.

4.6 Discussion

The following are the final considerations and conclusions for all comparisons of the strategies carried out.

4.6.1 Comparison between Full-Threshold strategies: 4-2 and 4-2-1

The results obtained show that both strategies are excellent in two different characteristics. The 4-2 strategy less precise but with a smaller amount of projections and vice versa the 4-2-1 strategy more precise but with a higher number of projections.

It is necessary to consider the request of the patient who performs the diagnostic examination: the 4-2 strategy, although having a lower number of projections, takes several minutes (11 minutes more or less) to acquire the thresholds of each point of the grid, therefore the 4-2-1 strategy with a high number of projections is to be excluded. Considering also that the error that differentiates the two strategies differs by an acceptable value, the Full-Threshold 4-2 strategy is usually taken into consideration.

In order to determine which strategy is the best, it is always necessary to consider the request and needs of the patient under examination: a diagnostic examination that is too long (more than 10 minutes) and requires the patient's attention will never be successful. Therefore, it is usually considered the fastest but less precise strategy.

4.6.2 Comparison between Full-Threshold 4-2 strategy and Zest strategy

Considering what is written above, there are clear differences in this case.

The two strategies compared are no longer similar: they have been implemented with a completely different algorithm. On the one hand the Full-Threshold that always uses the same dB increment/decrement at all points of the grid, and on the other hand the Zest that instead is based on Bayesian algorithm converted into binary decision trees that projects different intensities at each point of the grid.

The trend both considering the MSE and the number of projections is very different for both the two strategies.

The results obtained show that the Zest is clearly superior to the 4-2 strategy both in terms of acquisition time (defined in number of projections) and in precision (defined in MSE).

For this reason, within COMPASS this strategy is much more used: it allows an examination that lasts less and is also more precise.

The Zest is better than the Full-Threshold strategy because they are considered a priori characteristics of the patients under examination: in this way it is possible to "skip" passages when different light intensities are projected. With the 4-2 strategy all the points of the grid are tested in the same way with the same algorithm (adding or subtracting the same value of dB, not considering the average of threshold in that point); with the Zest each point of the grid is associated to a zone that, considering the age of the patient, has a particular light sensitivity. It is therefore easier to start from that intensity and then adjust a few dB to find the threshold.

In short, thanks to an algorithm based on a priori probability, the Zest is able to estimate the threshold in a more precise way in less time.

4.6.3 Comparison between Zest strategy and Zest strategy with cc

This case is very similar to the comparison between the two Full-Threshold 4-2 and 4-2-1 strategies because it is a comparison of two strategies that have the same algorithm but with a small difference.

The Zest cc differs from the Zest because controls were introduced at the beginning of the projections to obtain a more accurate diagnostic examination. From the graphs previously analysed we can see that there are very small differences between the two strategies: Zest with cc results to have a higher number of projections because more nodes are added in the tree, but it is more precise. Considering also that the number of projections, even if greater, differs little from the Zest, it can be deduced that the Zest cc is a good compromise for acquisition time and precision. For this reason, it is certainly more used in diagnostic tests with COMPASS.

In conclusion, through the simulation of virtual patients, it was possible to validate what happened without virtual patients. The performance of different strategies was compared in order to obtain the best result for the diagnostic test.

Conclusion

The results obtained with the thesis project were satisfactory because they reflected what happens in reality with non-virtual patients.

This new method for the comparison of visual field acquisition strategies is useful for performance evaluation during the implementation of future strategies.

The main features that have been assessed correspond to the current needs of patients performing the diagnostic examination: acquisition time and accuracy of the results obtained.

With the simulation of virtual patients, it was possible to eliminate the subjectivity factor typical of the examinations of these medical devices (in this case COMPASS has been considered).

The strategies chosen for the performance evaluation have been implemented through MATLAB and correspond to Full-Threshold 4-2 and 4-2-1, Zest and Zest with control. Comparisons were made between two different strategies to evaluate positive and negative aspects of both and to identify the best compromise (in terms of error and acquisition time). The strategy that satisfy the specifications was Zest with cc (control).

In the model, healthy virtual patients (whose data are the result of a clinical trial at the San Paolo Hospital in Milan) and not glaucomatousis were considered. It has not yet been possible to simulate the progression of glaucoma: this serious degenerative disease advances in a completely unpredictable and irregular way. Consequently, there are no virtual glaucomatousis patients in the model, also due to lack of data.

In future developments, with eye screening and examinations it will be possible to collect sufficient data to try to simulate the progression of glaucoma and then also sick patients can be considered within the model.

The method created is versatile: any type of strategy of any algorithm can be tested on it, because given the input of the algorithm definition related to a particular strategy, it is able to calculate the performance of the latter. In this way it will be possible to optimize the costs of clinical trials for the authentication of strategies and the implementation of new strategies will be easier. In fact, the new method defined by this thesis will not only allow to compare performances in a faster way but will refer to results obtained by virtual patients completely eliminating the subjectivity of the examination.

Bibliography

[1] David B. Hanson, "*Visual Fields*", Butterworth Heinemann, 1994, GML;

[2] G. Sini, "*L'occhio umano nella maggioranza dei vertebrati*", Riferimenti agli articoli O3, "*Le lenti sferiche*", O 12, "*L'occhio*" (della serie "Ottica sperimentale") ed A5 ("L'evoluzone biologica", pag. 55−59);

[3] Anastasi G., "*Trattato di Anatomia Umana*", edi-ermes, 2010, Milano;

[4] Netter FH., "*Atlante di anatomia umana*", 2001, Masson;

[5] Heike Kroeger, Wei-Chieh Chiang, Julia Felden, Amanda Nguyen, and Jonathan H.Lin, "*ER stress and unfolded protein response in ocular health and disease*", FEBS J. 2019 January; 286(2): 399–412. doi:10.1111/febs.14522;

[6] Janis T. Eells, "*Mitochondrial Dysfunction in the Aging Retina*", Biology, 2019, 8, 31; doi:10.3390;

[7] Purves D, Augustine GJ, Fitzpatrick D, et al., "*Neuroscience*" 2nd edition, 2001, Sunderland (MA): Sinauer Associates;

[8] Lyne Racette, Monika Fischer, Hans Bebie, Gábor Holló, Chris A. Johnson, Chota Matsumoto, "*Visual Field Digest*", Editor:Haag-Streit AG, 2016, Köniz, Switzerland, 6th Edition;

[9] Natalie Schellack, Gustav Schellack, Selente Bezuidenhout, "*Glaucoma: a brief review*", S Afr Pharm J, 2015, 82(5):18-22;

[10] Tham Y, Li X, Wong T, et al., "*Global prevalence of glaucoma and projections of glaucoma burden through 2040: a systematic review and meta-analysis*". Ophthalmology. 2014;121(11): 2081-2090;

[11] Parker J. Williamsa, Sherveen Saleka Robert, A. Prinzib Chris Bergstrom G. Paker Hubbard IIIa, "*Distribution patterns of torpedo maculopathy: Further evidence of a congenital retinal nerve fiber layer-driven etiology*", Saudi Journal of Ophthalmology, Volume 33, Issue 3, July–September 2019, Pages 260-267.

[12] David C Broadway, "*Visual field testing for glaucoma – a practical guide*", Community Eye Health Journal, 2012,Volume 25 ISSUES 79 & 80.

[13] William F. Hoyt, Lars Frisen and Nancy M. Newman, "*Fundoscopy of nerve fiber layer defects in glaucoma"*, Investigative Ophthalmology,November 1973,Volume 11: 815-829.

[14] Robert N. Weinreb, MD, Tin Aung, MD, PhD, and Felipe A. Medeiros, MD, PhD, "*The Pathophysiology and Treatment of Glaucoma*", JAMA, 2014 May 14; 311(18): 1901–1911. doi:10.1001/jama.2014.3192.

[15] Dr. Robert Cubbidge, "*Essentials of visual field assessment*", Optician 2012; 14-18;

[16] Lascaratos J, Marketos S. "*A historical outline of Greek ophthalmology from the Hellenistic period up to the establishment of the first universities*". Doc Ophthalmol 1988; 68:157–69;[17] Thompson HS. "*How visual field testing was introduced into office ophthalmology*",1993, David G. Cogan Ophthalmic Historical Society Meeting.

[18] Von Graefe A., "*Ueber die Untersuchung des Gesichtsfeldes bei amblyopischen Affectionen"* Graefes Archiv fur Ophthalmologie 1856; 2(Pt 2):258–98;

[19] U.Schiefer, J. Patzold,F. Dannheim, P.Artes, W.Harts, "*Conventional Perimetry*", Der Ophtalmologe 2005, 102(6): 627-646.

[20] Allison M McKendrick, "*Recent developments in perimetry: test stimuli and procedures*", Clinical and experimental Optometry, 2005; 88: 2: 73–80.

[21] Boel Bengtsson et al., "*A new generation of algorithms for computerized threshold perimetry, SITA*", Acta Ophthalmol. Scand. 1997: 75: 368-375.

[22] Moustafa Yaqub, "*Visual fields interpretation in glaucoma: a focus on static automated perimetry*", Community Eye Health Journal, 2012, Volume 25, Issues 79,80: 1-8.

[23] Douglas R. Anderson, Vincent Michael Platella, "*Perimetria Computerizzata*", 2000 Verduci editore.

[24] R Susanna Jr, R M Vessani, L Sakata, L C Zacarias, M Hatanaka, "*The relation between intraocular pressure peak in the water drinking test and visual field progression in glaucoma*", Br J Ophthalmol 2005;89:1298–1301. doi: 10.1136/bjo.2005.070649.

[25] Andrew J. Anderson, "*Utility of a dynamic termination criterion in the ZEST adaptive threshold method*", Vision Research 43, (2003) 165–170.

[26] Algis J. Vingrys, FAAO, Micheal J. Pianta, "*A new look at threshold estimation algorithms for automated static perimetry*", Optometry and Vision Science, August 1999, Vol. 76, No 8, 588-595.